Azoreduction:
Reductive Metabolism of Azo Food Dyes by Species of the Human Gut Microbiome

by

Riley Elder

A Thesis

presented to

The University of Guelph

In partial fulfilment of requirements
for the degree of

Master of Science

in

Molecular and Cellular Biology

Collaborative Specialization in Toxicology

Guelph, Ontario, Canada

ABSTRACT

METABOLISM OF AZO DYES BY
AZO REDUCTASES IN THE HUMAN GUT MICROBIOME

Riley Elder
University of Guelph, 2022

Advisor(s):
Dr. Emma Allen-Vercoe
Dr. P. David Josephy

Azo dye food colourants are widely used in Canada and other countries. When ingested, these dyes may be reduced by azoreductases of the gut microbiome bacteria to metabolites that might have immune-, neuro-, or genotoxic effects. I have identified obligate anaerobic bacterial species from the human gut that reduce these azo food dyes. Bacterial species representing six phyla were derived from human fecal microbiomes. Bacteria were incubated on dye-infused plates and decolourization was monitored by visual inspection. Taxa exhibiting high azoreductase activity belonged to the genera *Clostridium*, *Hungatella*, *Enterocloster*, *Veillonella*, *Dielma*, *Eggerthella*, *Odoribacter*, and *Phocaeicola*. The effects of the dyes on bacterial growth were studied. The genome sequences of two *Veillonella* spp. with high azo dye reduction activities were examined. Candidate genes were cloned and expressed as recombinant proteins, but none showed detectable azo dye reduction activity in vitro.

ACKNOWLEDGEMENTS

Firstly, I would like to thank my two advisors, Dr. David Josephy and Dr. Emma Allen-Vercoe for providing me with their wisdom, giving me their time, and being very supportive throughout my degree (and in a pandemic!). I am honored to be Dr. David Josephy's last graduate student and to have been so warmly welcomed into Dr. Emma Allen-Vercoe's lab. I'd like to thank my committee member Dr. Jennifer Geddes-McAlister, for her insight and encouragement. I greatly appreciated the ideas and morale boost from our international collaborators, also known as "Team Tartrazine", including Dr. Ali Ryan, Dr. Robert Keyzers, Dr. Joanne Harvey, Dr. David Ackerley, and Dr. Libusha Kelly.

Thank you to the members of the Josephy and Allen-Vercoe labs for helping me learn new techniques, giving me valuable advice, and for being a great community of scientists. The lab often felt more like a family rather than coworkers. I'd also like to give thanks to my friends on the second floor for always lending an ear to my troubles, brainstorming with me, and sharing many laughs together. I don't know how I would have made it through without the support!

A special thanks to all my friends who stuck by me throughout my life and degree, and for always having my back through thick and thin. My deepest appreciations go to my husband for believing in me and pushing me to be the best version of myself, as well as to my parents and sister for always providing me comfort and support.

TABLE OF CONTENTS

LIST OF TABLES

LIST OF FIGURES

LIST OF ABBREVIATIONS

ADI - Acceptable Daily Intake
ALT – Alanine Transaminase
AST – Aspartate Aminotransferase
BHI – Brain Heart Infusion medium
BLAST - Basic Local Alignment Search Tool
b.w. - Body Weight
CFU - Colony Forming Units
DAB - *p*-Dimethylaminoazobenzene
DCPIP – 2,6-Dicholophenolindophenol
ddH2O double-distilled water
EDTA - Ethylenediaminetetraacetic acid
EFSA - European Food Safety Authority
FAA - Fastidious Anaerobic Agar
FAO – Food and Agriculture Organization
FD&C – Federal Food, Drug and Cosmetic Act
FDA - Food and Drugs Act
IARC – International Agency for Research on Cancer
IMAC - Immobilized-metal-affinity chromatography
IPTG - Isopropyl beta-D-1-thiogalactopyranoside
JECFA – Joint FAO/WHO Expert Committee on Food Additives
LB - Lysogeny Broth
MW – Molecular Weight (kDa)
NADH – Reduced Nicotinamide Adenine Dinucleotide
NADPH – Reduced Nicotinamide Adenine Dinucleotide Phosphate
OD – Optical Density
OD 600 - Optical Density at 600nm wavelength
PCR - Polymerase Chain Reaction
rRNA – ribosomal Ribonucleic Acid
ROUT – Robust Regression and Outlier Removal
RMSD – Root-mean-squared Deviation
TAE – Tris-acetate-EDTA buffer
TSA - Tryptic Soy Agar
TSB - Tryptic Soy Broth
S (16S) - Svedberg sedimentation coefficient
S9 - Supernatant fraction from a homogenate, containing cytosol and microsomes
SDS-PAGE – Sodium Dodecyl Sulphate Polyacrylamide Gel Electrophoresis
sp. - Species
spp. - Species (plural)
SSU rRNA - Small Subunit ribosomal Ribonucleic Acid
WHO – World Health Organization

LIST OF APPENDICES

1 Literature Review and Research Objectives

1.1 Introduction

Dyes have been used by humans for centuries in materials such as foods, pharmaceuticals, cosmetics, textiles, and plastics[1]. They can be used for improving the appearance of foods, adding colour to colourless products, and allowing consumers to identify products (especially drugs) on sight[2]. Until the 19th Century, all dyes came from natural sources, such as vegetable extracts and animal products; however, these materials only gave limited colours and faded easily[3]. The synthetic dye industry began with the invention of the first synthetic dye in 1856[4]. While William H. Perkin was attempting to synthesize the anti-malarial drug quinine, he discovered that when aniline was oxidized, using nitric and sulphuric acids, a purple colour was produced[4]. The purple compound was a phenazine dye, which Perkin named mauveine (Figure 1.1)[4]. This was the first industrially produced synthetic dye, and it had rapid commercial success[4]. Synthetic dyes rapidly began to replace natural dyes due to their quick synthesis and colour stability, making them a more economical option in comparison to natural dyes[5].

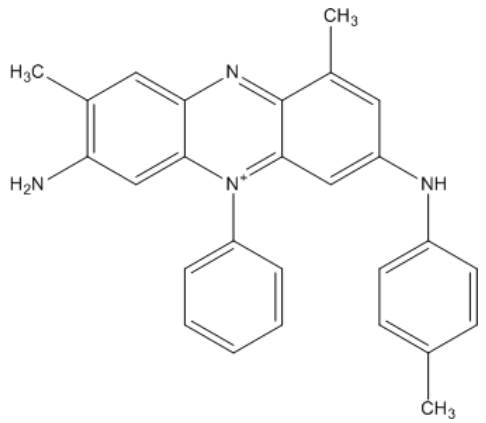

Figure 1.1: The structure of the dye mauveine, synthesized by William Henry Perkin in 1856[4]. (The structure was not determined until much later)

1.1.1 Azo Dye Structure

Dyes are coloured substances that, when applied to products, adhere by the formation of covalent bond, mechanical retention, or physical adsorption[6]. The colour of the dye is determined by the ability of the structure to absorb light within the visible range (400-700 nm)[3]. Chromophores are functional groups in the dye structure that absorb light, typically groups that are aromatic or have conjugated bonds, such as, nitro, azo or quinoid groups[3]. The colour is caused by the excitation of valence π electrons[3]. Azo dyes are characterized by one or more azo bonds [R-N=N-R][7]. This double-bonded nitrogen structure allows for azo dyes to produce brilliant colours[7].

Today, synthetic azo dyes are still widely used in pharmaceutical products, cosmetics, and food products[8]. The annual use of azo dyes in food processing is estimated at one million tons globally[9]. Even though select azo dyes have been approved by food regulatory agencies, food items containing synthetic colour have been increasingly avoided by consumers due to concern about possible health effects[8]. The chronic effects of azo dye ingestion have been studied for several decades, given that the reduction of these dyes by microbes can lead to the formation of toxic products, such as aromatic amines[8]. Since the human intestinal tract has a large and diverse community of microbes, the metabolites produced by azo dye degradation should be of concern with regard to the safety of the use of dyes food products[8].

1.1.2 Azo Dye History

The first azo compounds were synthesized by Johann Peter Griess, who discovered that aniline could react with nitrous oxide, forming a compound with twice as much nitrogen[4]. Griess then coupled these diazo compounds with aromatic compounds to create a double bonded nitrogen (N=N) link between the aromatic groups, giving rise to bright colours which are

characteristic of azo dyes[4]. Griess' discovery led to the first azo dye, aniline yellow, which was manufactured in 1861, with the colour Bismark Brown following in 1863 (Figure 1.2)[3]**.** The German chemist Bottiger used Griess' chemistry to form a *bis*-diazo compound derived from benzidine, which produced Congo Red, the first benzidine-based azo dye (Figure 1.3)[4]. The 1890s became the 'mauve decade', where the chemical dye industry flourished and synthetic dyes almost wholly replaced natural dyes[3]. The production of synthetic benzidine dyes spread from Germany to England and the United States[4]. In 1895, Dr. Ludwig Rehn reported the dangers of aniline production after observing a relationship between workers producing aniline and the development of bladder cancer, seeing more than 50 cases among dye industry workers in the Frankfurt area[4]. Few occupational hygiene measures were taken regarding chemical industry workers until after World War II, where subsequent studies linked benzidine exposure to a 60-fold increased risk of bladder cancer compared to non-exposed controls[4]. The cancer was likely caused by aromatic amines, such as benzidine, that were being produced in the dye factories[4]. This discovery made it apparent that legislation needed to control dye manufacturing. By the 1950s, it was accepted that benzidine was a significant occupational hazard as a bladder carcinogen[4]. When benzidine-based azo dyes are ingested, they are reduced to aniline and benzidine by the action of azoreductase enzymes in the gut[4]. The metabolism of azo dyes may generate toxic products.

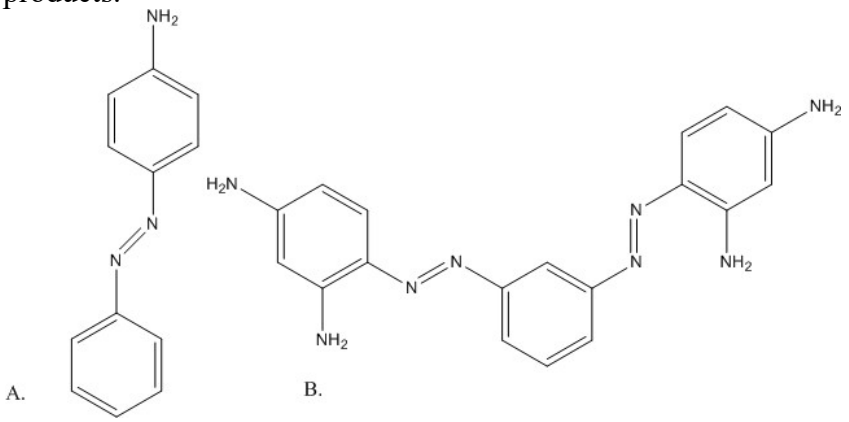

Figure 1.2: The structures of Aniline Yellow (A) and Bismarck Brown (B)[1].

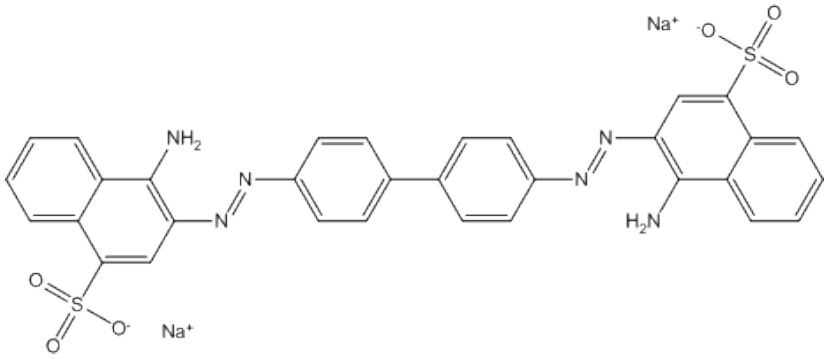

Figure 1.3: The structure of Congo Red[3].

1.2 Azo Dyes: Regulatory Aspects

Government regulation of azo dyes began in 1883 with the work of Harvey W. Wiley, the head chemist at what is now the U.S. Department of Agriculture[10]. He was known as the "Father of the Pure Food and Drugs Act", 1906[10]. This act originally listed seven coal-tar dyes as safe for use in Food, Drug, and Cosmetic (FD&C) Dyes (Table 1.1)[10]. Ten more dyes were added between 1916-1929, including Methyl Yellow (Table 1.2)[10]. Methyl Yellow (N,N-dimethylaminoazobenzene, DAB) was first used as a food additive in 1918 (Figure 1.4)[11]. In 1948, James and Elizabeth Miller discovered that its metabolite 4-monomethyl-aminobenzene cause liver tumours in mice[12]. This discovery led to the investigation into the carcionogenic bio-activation of conjugated dyes[11]. In 1975, 32 synthetic dyes were permitted for food use by UK legislation, but by 1973, 19 of these dyes had been removed due to toxic effects[10,13]. Azo dyes may be "pro-toxicants", where the parent compound may not itself be toxic, but can be bio-transformed into metabolites (e.g. colourless aromatic amines) that are[1].

Table 1.1: Coal tar dyes considered safe FD&C dyes in 1906[10].

Common dye name	FD&C name	Azo dye (X)	Date delisted
Ponceau 3R	Red No. 1	X	1961
Amaranth	Red No. 2	X	1976
Erythrosine	Red No. 3	-	-
Indigotine	Blue No. 2	-	-
Light green SF	Green No. 2	-	1966
Naphthol yellow	Yellow No. 1	-	1959
Orange 1	Orange No. 1	X	1959

Table 1.2: Azo dyes added to the FD&C list between 1916-1929[10].

Common dye name	FD&C name	Azo dye (X)	Date listed	Date delisted
Tartrazine	Yellow No. 5	X	1916	-
Sudan I	-	X	1918	1918
Butter Yellow	-	X	1918	1918
Yellow AB	Yellow No. 3	X	1918	1959
Yellow OB	Yellow No. 4	X	1918	1959
Guinea Green B	Green No. 1	-	1922	1966
Fast Green FCF	Green No. 3	-	1927	1959
Brilliant Blue FCF	Blue No. 1	-	1929	-
Ponceau SX	Red No. 4	X	1929	1976
Sunset Yellow FCF	Yellow No. 6	X	1929	-

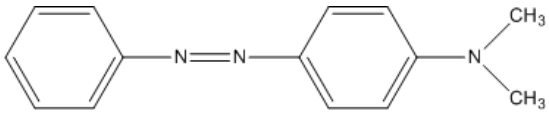

Figure 1.4: The structure of butter yellow (Methyl Yellow)[11].

1.3 Azo Dye Food Safety

Today, azo dyes are the largest group of colorants produced worldwide, both in volume and number, constituting approximately 70% of all organic dyes[14]. The popularity of azo dyes is attributed to their simple synthesis, structural diversity, high molar extinction coefficients, and photolytic and chemical stability (making them resistant to fading)[3]. Food dye safety remains a major issue around the world. Currently, Canada allows only four azo dyes to be used in food products: Amaranth, Allura Red, Sunset Yellow and Tartrazine (Figure 1.5)[15]. All of the permitted azo dyes are sulphonated compounds, giving better water solubility. Sulphonated compounds are easily excreted in urine, which may lessen any toxic effects. The European Food Safety Authority (EFSA) is currently investigating whether certain food dyes increase hyperactivity in children[10]. If this concern is substantiated, manufacturers may have to abandon the use of Tartrazine, Sunset Yellow, Allura Red, Quinoline Yellow, Ponceau 4R and Carmoisine (Figure 1.5, Figure 1.6) (Table 1.3) in their products[10].

Table 1.3: Synthetic azo dyes used in food products: FDA names, common names, E numbers and molar masses[15].

Common dye name	FDA name	E number	Molar Mass
Allura Red[b]	FD&C Red No. 40[a]	E-129	496.43
Tartrazine[b]	FD&C Yellow No. 5[a]	E-102	534.37
Sunset Yellow[b]	FD&C Yellow No. 6[a]	E-110	452.37
Amaranth[b]	FD&C Red No. 2	E-123	604.47
Ponceau SX[b]	FD&C Red No. 4	-	480.43
Ponceau 4R	-	E-124	604.47
Carmoisine	FD&C Red No. 10	E-122	502.434
Quinoline Yellow	D&C Yellow No. 10	E-104	579.42

a – dyes approved by the United States FDA

b – dyes approved for use in Canada

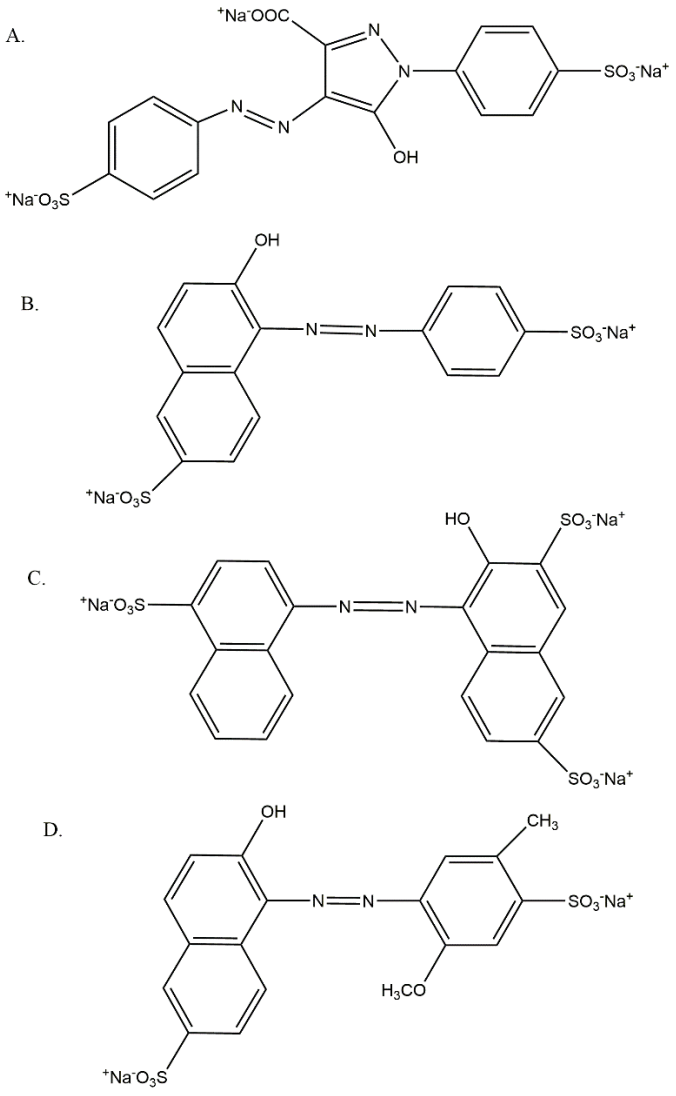

Figure 1.5: The structures of Tartrazine (Yellow No. 5) (A), Sunset Yellow (Yellow No. 6) (B), Amaranth (Red No. 2) (C), and Allura Red (Red No. 40) (D)[10].

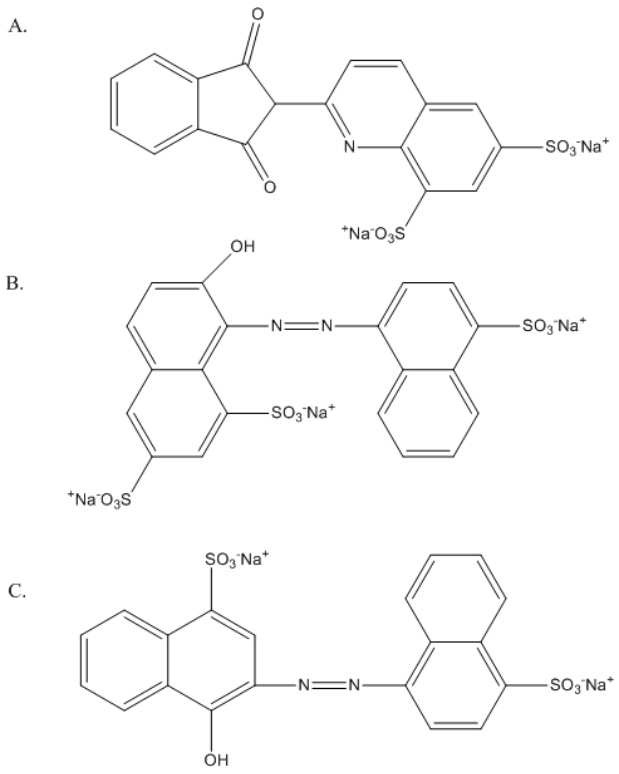

Figure 1.6: The structures of Quinoline Yellow (A), Ponceau 4R (B) and Carmoisine (C)[10].

1.3.1 Amaranth

The azo dye Amaranth (FD&C Red No. 2 and E123) is still used commonly, although Soviet scientists determined in 1969 that the long-term use of this dye caused cancer in laboratory animals (Figure 1.5)[10]. In 1976 the FDA banned Amaranth, while Canadian regulators concluded that there was insufficient evidence to justify removal of the dye from food[10]. In 1984 the estimated ADI for Amaranth was determined as 0.5 mg/kg by the Joint FAO/WHO Expert Committee on Food Additives (JECFA). In 1994, Sweeney *et al*. found that both Amaranth and Sunset Yellow metabolites did not mutate *S. typhimurium* strains TA100 and TA98, but did mutate TA102, suggesting both compounds may cause oxidative mutagenesis[16]. When reduced

by repair-deficient *E. coli,* Sunset Yellow and Amaranth induced DNA damage[16]. The EFSA determined that the ADI for Amaranth should be lowered to 0.15 mg/kg bw when re-evaluated in 2010. It was determined by the EFSA that at the 97.5th percentile of consumption of food colouring, the predicted exposure to Amaranth may be as much as 6 times higher than the ADI of 0.15mg/kg bw, suggesting it is likely that an individual will exceed the ADI for Amaranth. This is compounded by the fact that in Canada, food products do not have to list the amount of dye content.

1.3.2 Allura Red

Allura Red, also known as FD&C Red No. 40 or E129, is a synthetic red azo dye commonly used as a food colourant (Figure 1.5). This dye was evaluated in 1981 by JECFA to have an ADI of 7 mg/kg; the ADI was re-evaluated in 2016 and was not altered. In 2009, Shimada *et al*. found that Allura Red and Amaranth caused colon-specific DNA damage in mice[17]. Mice were administered 1-10 mg/kg dye via gavage. Brain, liver, kidney, glandular stomach, colon, urinary bladder and bone marrow were sampled 3 h after treatment[17]. The comet assay showed DNA damage for colon cells of the mice 3 h after Allura Red and Amaranth administration at 10 mg/kg[17]. This result was not seen when a corresponding study was conducted in rats with up to 1000 mg/kg dye administered[17]. These results match the inconclusive results by the Working Group of IARC for Amaranth toxicity in mice, rats, and dogs[17]. Allura Red has not been found to be carcinogenic in rats or mice but showed evidence of behavioural and physical toxicity in developing rats[18]. Vohrees *et al*. discovered that exposure to Red 40 led to decreased wheel activity in rats, which contrasts with the hyperactivity reported in children[19]. In 2021, He *et al*. discovered that in mice with over-expression of IL-23, Allura Red and Tartrazine metabolism induced colitis, and that its induction was contingent on the reduction of the dyes by the commensal microbiota[20].

1.3.3 Sunset Yellow

The ADI of azo dye Sunset Yellow FCF (FD&C Yellow 6 or E 110) was determined to be 2.5 mg/kg body weight (bw), which was established in 1982 by JECFA; the value was re-evaluated in 2011 and changed to 4 mg/kg bw. In 2009, the EFSA lowered the ADI to 1 mg/kg bw, and then the EFSA increased the ADI to 4 mg/kg bw, to be consistent with the ADI set by JECFA.

It is speculated that Sunset Yellow, Allura Red and Tartrazine cause hyperactivity in children. The first study to link hyperactivity in children with synthetic food colourants was published by Feingold in 1975[21]. Later, McCann *et al*. performed a randomized, double-blind, placebo-controlled, crossover trial to test the relation between hypersensitivity in children and consumption of food colour additives[22]. Two drink mixes (drink mix A and drink mix B) were given to children and hyperactivity was monitored, drink mix A included: 5 mg Sunset Yellow, 2.5 mg Carmoisine, 7.5 mg Tartrazine and 5 mg Ponceau 4R, and drink mix B included: 45 mg sodium benzoate, 7.5 mg Sunset Yellow, 7.5 mg Carmoisine, 7.5 mg Quinoline Yellow and 7.5 mg Allura Red[22]. Both drink mixes increased hyperactivity in the children; however, this could have been a result of the sodium benzoate preservative or the artificial colours, since the control drink did not include the sodium benzoate preservative[22]. In 2020, El-Borm *et al*., demonstrated that Sunset Yellow and Tartrazine induced apoptosis and DNA damage when administered *in ovo* of 1.575 or 0.375 mg/egg during the organogenesis phase of the chick embryo[23]. These dyes may have teratogenic effects at high doses and should be re-evaluated by the JECFA[23]. In 2009, the EFSA published a scientific opinion on the re-evaluation of Sunset Yellow stated that in the general European population, refined intake is typically below the temporary 1 mg/kg bw ADI. However, in 1–10-year-old children the mean and high percentile of exposure (97.5th) can be 0.6-5.8 mg/kg bw/day[24]. Products including azo dyes are heavily used in consumables targeted for children, such as soda and candy; this could be contributing to the consumption of azo dyes

by some children above the ADI recommendations.

1.3.4 Tartrazine

Tartrazine, also known as FD&C Yellow No. 5 or E102 in Europe, is a synthetic yellow azo dye commonly used as a food colourant (Figure 1.5)[15]. Tartrazine is found in soft drinks, sports drinks, flavoured chips, sauces, ice creams, chewing gums, and non-food consumables such as vitamins, cosmetics, soaps, shampoos, and prescription medications[15]. The ADI for Tartrazine is 7.5 mg/kg bw/day, which would be the equivalent of 225 mg per day for a 30 kg child. Early studies showed that this food dye is safe to consume at the ADI, since no harmful effects were observed in human or experimental models[25]. In many Ames test studies, with or without S9 enzymes, it was also shown that Tartrazine was not mutagenic with a daily intake of 7.5 mg/kg body weight[26]. Recent investigations have challenged the safety of Tartrazine, reporting that it can induce angio-edema, immunotoxic and genotoxic effects, exacerbations of asthma and urticaria in atopic patients[27]. Tartrazine may be responsible for triggering asthma and urticaria attacks, particularly in individuals who already have aspirin intolerance[27].

The genotoxicity of Tartrazine has been controversial because of the varying results in studies. Many studies on mutagenicity have demonstrated that Tartrazine has no mutagenic potential, yet other more recent studies have revealed genotoxicity[26]. Tartrazine was shown to induce chromosomal aberrations in Chinese hamster cells by Ishidate *et al.* in 1981 as well as in rat somatic cells by Giri *et al.* in 1990[26,28]. However, in 1995, Durnev *et al.* did not observe chromosomal aberrations in mouse cells[29]. In a 2017 study, Khayyat *et al.* randomly divided 20 Wistar albino rats into two groups with Group 1 orally receiving 1mg/kg bw distilled water for 30 days and Group 2 orally receiving 7.5 mg/kg bw Tartrazine dissolved in water for 30 days[15]. Leukocytes were harvested from the rats and a comet assay was performed; when exposed to Tartrazine there was a significant increase in leukocyte DNA comet length, demonstrating

genotoxicity in tested cells[15]. Khayyat *et al.* also measured blood levels of serum ALT, AST and ALP, which were significantly elevated in the group that was administered Tartrazine, indicating liver damage[15]. The serum levels of creatine, urea and uric acid were also significantly elevated in the Tartrazine-administered group indicating kidney damage[15]. These results led Khayyat *et al.* to propose that the mechanism of damage is oxidative stress generated by Tartrazine metabolism[15].

1.3.5 Tartrazine Metabolism

In a 1962 publication, Daniel reported on the metabolism of Tartrazine administered to rabbits via a stomach tube[30]. He used paper chromatography to show that the part of the Tartrazine molecule originating from sulphanilic acid was excreted in the urine as sulphanilic acid (74%) and N-acetylsulphanilic acid (22%), demonstrating that the Tartrazine molecule underwent a reductive fission[30]. In the same year, Ryan and Wright reported that when they gave small amounts of Tartrazine to rats intraperitoneally, no amine metabolites were detected in the urine[30]. This finding indicates that reductive cleavage of Tartrazine did not take place after intraperitoneal administration, suggesting that orally administered Tartrazine is metabolized mainly by the intestinal microbiota rather than in the liver[30].

In 1964, Jones, Ryan and Wright conducted a study on the excretion of sulphanilic acid in animals and humans given Tartrazine but did not document any other metabolites[30]. In 1965, Westöö studied the metabolism of Tartrazine in rats and found a different metabolite from the pyrazolone part of the Tartrazine molecule[30]. Westöö discovered that rats given Tartrazine via gastric intubation at 0.03-0.3 g/kg bw produced feces of normal colour immediately after excretion, but, following air exposure, the fecal pellets acquired a violet tinge. The rats were sacrificed and dissected 4-16 h after Tartrazine administration; the caeca changed to violet when exposed to air. However, the small intestine did not show any violet colouring. When the violet compound in the feces was extracted with water at room temperature, there was a colour shift in

the solution from violet to red. The violet products showed stability at pH 7.0-8.5 and the same absorption wavelengths of light (maxima and minima) as the compound 4-amino-5-oxo-1-(*p*-sulphophenyl)-2-pyrazoline-3-carboxylic acid (Figure 1.7). Under a N_2 atmosphere, no violet compound is formed (Figure 1.7). Therefore, the violet product was proposed to have the structure produced from taking up an oxygen molecule and expelling ammonia (Figure 1.7). Westöö's metabolite (Figure 1.7.1) is the speculated product of aerobic Tartrazine metabolism; the structure has not been proved definitively. In 2008, Perez-Diaz and McFeeters used *Lacticaseibacillus casei* and *Lacticaseibacillus paracasei* to aerobically metabolize Tartrazine [31]. The reduction metabolites were identified with liquid chromatography-mass spectrometry (LC-MS) analysis and a product that was 111 Da larger than the precursor molecule was found[31]. This product was purple under aerobic conditions and colourless under anaerobic conditions[31].

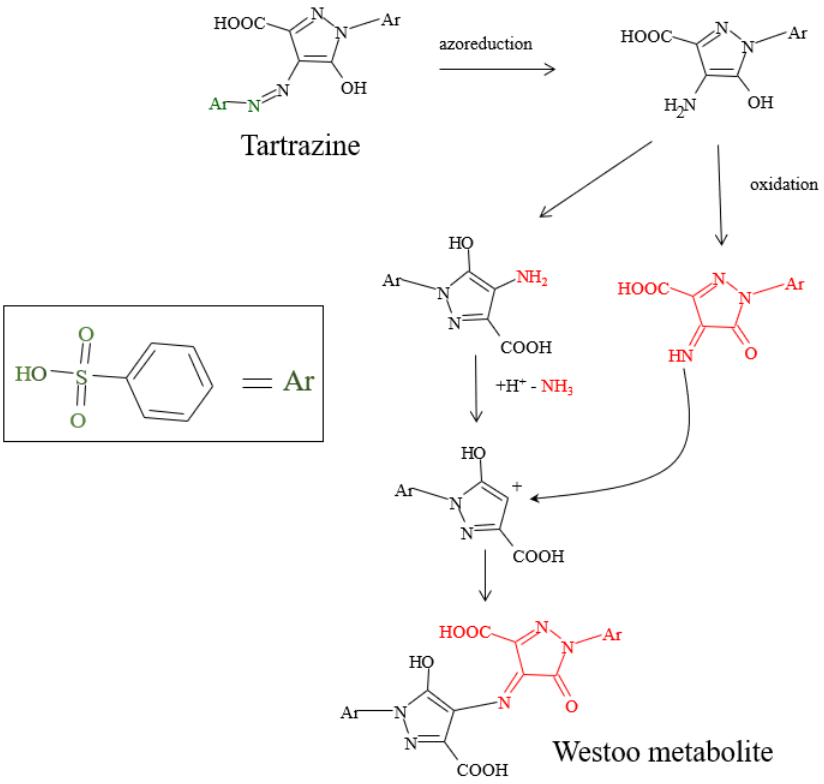

Figure 1.7: The proposed mechanism of Tartrazine metabolism in the rat intestinal tract[25].

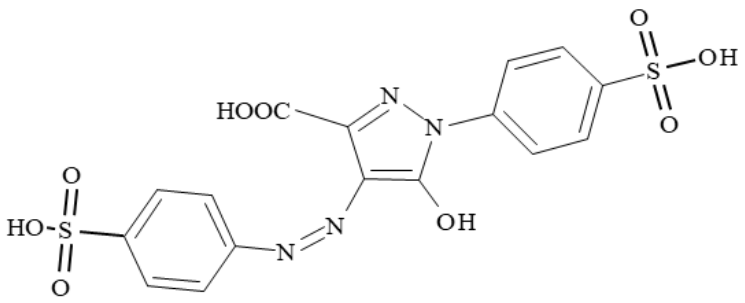

Tartrazine; $C_{16}H_{12}N_4O_9S_2$ 468.0 Da

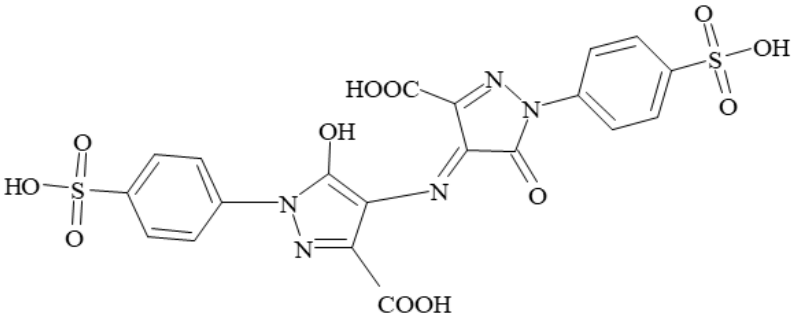

Westoo metabolite; $C_{20}H_{13}N_5O_{12}S_2$ 579.0 Da

Figure 1.7.1: The proposed structure of Westöö's metabolite compared to Tartrazine[30].

In 2017, Elbana *et al*. demonstrated that Tartrazine, Sunset Yellow, Carmoisine and Ponceau 4R are decolourized by multiple intestinal bacterial species, such as *Lactobacillus* spp*., E. coli, and Enterobacter* spp.[8]. In 1978, Chung *et al.* showed that Tartrazine, Sunset Yellow, Amaranth and Allura Red could be metabolized by certain strains of *Fusobacterium* sp*., Bacteroides thetaiotaomicron* and *Citrobacter* sp.[32]. In 1997, Rafii *et al.* obtained *Clostridium* spp. from the human intestinal tract and determined that these strains facilitated decolorization of Tartrazine, Sunset Yellow and Allura Red[7]. They then tested for mutagenicity in *S. enterica* Typhimurium

Ames test strains TA98 and TA100, which detect frame-shift mutations and base-pair substitutions or mutations[7]. At doses from 0.1-10 mg/plate, none of the dyes or their metabolites were mutagenic in the presence or absence of rat or hamster liver S9[7].

1.4 Mechanism of Azo Dye Metabolism

Since the 19th Century, the use of azo compounds in the environment and food products has increased substantially, with the dyestuff and textile industries being the largest producers of azo dyes[1]. It is estimated that 15% of all the dyes synthesized worldwide will enter the environment as industrial effluent[33]. Azo dyes can cause serious damage to aquatic ecosystems due to their photo-stability, resulting in high persistence causing water turbidity[11]. The metabolism of these compounds is facilitated by specific enzymes, 'Azoreductases'. Azoreductases are a family of diverse enzymes found in many bacterial species; homologues are present in eukarya[34]. These enzymes may be important for bioremediation to prevent accumulation of these dyes as pollutants[11].

1.4.1 Azoreductase

Azo bonds are mainly degraded through reductive mechanisms, caused by contact with microorganisms in the environment, by bacteria in a mammalian intestinal tract, or the liver[1]. In certain cases, azo dyes can also be degraded by peroxidases and oxidases through oxidative reactions[35]. The most common pathway of biological azo degradation is through a group of enzymes, azoreductases, which are flavoenzymes[34]. These enzymes have been characterized in aerobic and anaerobic bacteria as well as in eukaryotes such as yeast and mammals[34]. Three groups of azoreductases have been found and identified in a range of bacterial genera, including *Escherichia, Bacillus*, *Pseudomonas, Geobacillus, Lysinibacillus, Enterococcus, Eubacterium and Clostridium*[1,36–39]. Two of the three groups are flavin-dependent enzymes, classified into NADH-preferred and NADPH-preferred azoreductases, while the third group is flavin-free

azoreductase[1,36]. The flavin-dependent enzymes, such as *P. aeruginosa* (AzoR) or *Enterococcus faecalis* (AzoA), use the flavin (FMN or FAD) to transfer electrons from NAD(P)H to substrates[39]. The purported azoreductase reaction is a Ping Pong Bi-Bi mechanism, where the first electron transfer results in a hydrazone tautomer of the substrate (Figure 1.8)[40]. The second electron transfer to the substrate allows for the azo bond to be reduced completely[40]. The intestinal microbiota reduces azo dyes under anaerobic conditions via flavin-dependent azoreductases. Flavin-free NADPH-preferred azoreductases reduce azo bonds by simultaneously joining the substrate and electron donor together in the active site; then, a direct hydride transfer happens in the reaction center[36]. This binding mechanism purportedly has a high substrate specificity, where out of the 9 substrates tested, Orange I was the only compound reduced[36]. These enzymes have been purified from *Xenophilus azovorans* KF46F and *Pigmentiphaga kullae* K24[41]. Flavin-dependent azoreductases are more common and can metabolize almost all azo dyes, due to their broad substrate specificity[1].

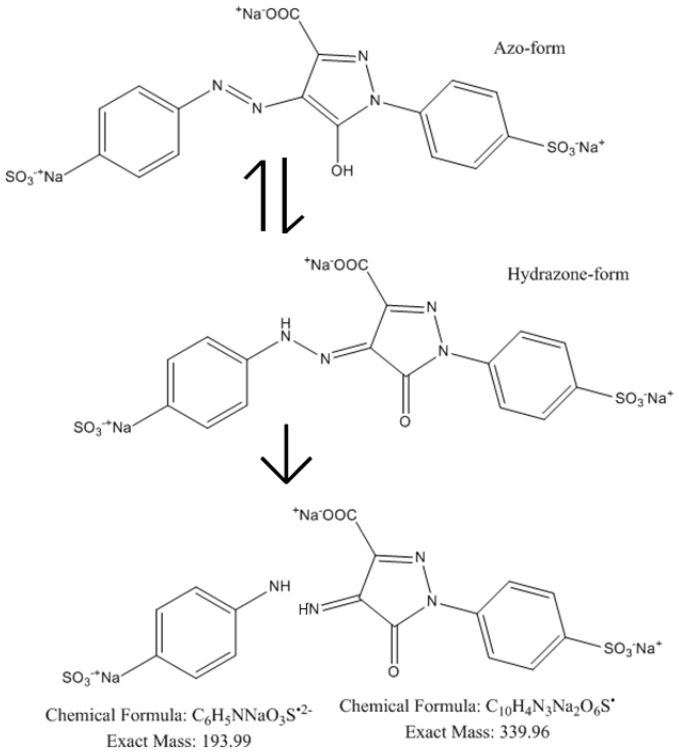

Figure 1.8: Formation of hydrazone tautomer of Tartrazine and its reduction to form two putative metabolites[40].

The biological role of these azoreductase enzymes remains uncertain, but has typically been attributed to the detoxication of antibacterial quinones produced by some plants[34]. These enzymes can reduce a broad range of substrates including nitrofurans, azo-compounds and quinones[34]. The mechanism of reduction explains the ability for azoreductases to reduce both quinone and azo substrates, potentially resulting in azoreductases being classified as NAD(P)H quinone oxidoreductases (NQOs)[40]. Mammalian azo reductases typically have very low sequence identity with bacterial enzymes, but they reduce both quinone and azo compounds[40].

1.4.2 Subcellular Localization

Much remains unknown concerning the mechanisms of the interactions of azo dye substrates with bacterial azoreductase enzymes. The debate whether the dyes are taken up by the cell or excreted into the environment is still ongoing and the outcome may be different depending on the organism. However, there is increasing evidence that these enzymes may be secreted. In 1990, Rafii *et al*. showed that azoreductase enzymes are secreted in the presence of azo dyes for the bacterial species *Eubacterium* spp., *Clostridium* spp., *Bacteroides* sp. and *Butyrivibrio* sp[42]. These species were isolated from the human intestinal microbiome and tested for the ability to reduce Direct Blue 5 or Nitro Red with dye-infused plates, crude protein extracts and supernatant extracts; the highest specific activity of supernatant extracts was seen for *C. perfringens* and *C. clostridiiforme*[42]. There was more enzyme in the supernatants than in the cell lysate, suggesting that the enzymes are extracellularly excreted[42].

In 2014 Morrison and John discovered and characterized a novel azoreductase in *Clostridium perfringens* (AzoC) that has a trimeric structure, whereas all other classified azoreductase enzymes have dimeric structures[43]. *C. perfringens* is an anaerobic microorganism that inhabits the human intestine and produces an azoreductase (AzoC), an NADH-dependent flavin oxidoreductase[43]. The authors stated that azoreductase secretion in *Clostridium perfringens* was in response to sulphonated azo dye exposure [44]. Through exposure studies, azo dyes were found to cause cytoplasmic protein release; sulphonation (negative charge) of azo dyes was key in facilitating protein release of AzoC and found to be dye-dependent [44]. AzoC was found to localize to the Gram-positive periplasmic region [44] This idea was supported by Rafii and Cerniglia in 1993, where the hypothesized azoreductase in *C. perfringens* was antibody labelled to identify the cellular localization of this protein, and it was observed that it was synthesized in the cytoplasm and then secreted[45].

1.4.3 Azoreductase Phylogeny

Recently there have been many advances in genome sequencing methods, such as small-subunit (SSU) rRNA (16S rRNA) gene sequencing or quantitative PCR coupled with denaturing gradient gel electrophoresis[1,46]. These techniques have given a better understanding of the roles of communal microbiota that are difficult to culture, including their mutualistic relationship with the host as well as associations with different diseases[46]. Azoreductases are ubiquitous among organisms and are found in prokaryotes (anaerobes and aerobes) as well as eukaryotes[47]. Bafana and Chakrabarti endeavoured to reconstruct the evolutionary history of the azoreductase enzyme family by comparing database azoreductase sequences with the phylogeny of the organisms obtained using SSU rRNA sequences[47]. For the analysis, sequences from nine bacterial, four mammalian and one yeast species were selected; both nucleic acid and protein acid sequences were obtained from Genbank[47]. Sequences of the conserved azoreductase domains were compared to the SSU rRNA phylogeny, taking into account the flavin nucleotide binding site, and the homology between similar species, bacterial or otherwise, was determined to be inconsistent[47]. Instead, it was discovered that the yeast azoreductase sequence aligned with prokaryotic sequences[47]. Several similarities were found between azoreductases of *E. coli, E. faecalis* and mammals, such as their NAD(P)-binding residues and the enzymes existing in dimeric form, and furthermore the flavin nucleotide binding residues were highly conserved in all azoreductases[47]. It is proposed that azoreductases originated in prokaryotic cells and were laterally transferred from ancient Bacillota (Firmicutes), through a series of isolated events, to yeasts and mammals[47].

1.4.4 The Gut Microbiota

The human intestinal tract plays a large role in degrading xenobiotics into metabolites, some of which can cause genotoxicity or carcinogenicity[1]. Human exposure to azo dyes can

occur through inhalation, skin contact or ingestion[48]. If ingested, azo dyes can be bio-transformed into colourless aromatic amines which may be carcinogenic[48]**.** Despite the fact that azo dye-containing textiles, food colourings and pharmaceuticals have been used for over 150 years, understanding of the organisms – and the specific enzymes - that metabolize these molecules[49] remains incomplete. There has been little characterization of azoreductase enzymes in human gut bacterial species that show azoreductase activity[49]. Azoreductase activity has been studied for different species of facultative anaerobes, such as *Escherichia coli, Pseudomonas aeruginosa, Bacillus spp., and Enterococcus spp.*[50 43]. Azoreductase activity has also been studied for many obligate anaerobic species *Clostridium* spp*., Eubacterium* spp*., Fusobacterium* spp*., Sphingomonas* spp*., Citrobacter* sp*., Bifidobacterium* spp*., Coprococcus* sp*., Peptostreptococcus* spp*., Veillonella parvula, Acidaminococcus* sp*., and Bacteroides* spp.[11,43,50,51]. However, enzyme characterization has been mainly carried out for facultative anaerobic bacteria, whereas obligate anaerobic species have been largely ignored[43].

It is believed that bacterial isolates may vary in their ability to reduce different dyes, meaning that the toxic effects of azo dyes could be contingent on the dye-reducing species present and the structure of the dye[49]. The most common bacterial species in our intestines are anaerobic members of the Bacteroidota (Bacteroidetes) and Bacillota phyla [52]. Included within the Gram positive Bacillota phyla, are the Clostridia class and the Enterococcaceae and Lactobacillaceae families[1]. Some tested members of these groups are more active at reducing certain azo dyes than others, and toxic metabolites can occur in the gut depending on the ingested dye. Other species that comprise fewer than 10% of the intestinal microbiota are included in the phyla Actinobacteria, Fusobacteria, Proteobacteria and Verrucomicrobia[1]. The majority of azoreductase research has focused on facultative anaerobic bacteria (and especially members of Proteobacteria) with minimal work reflecting strictly anaerobic bacteria in the human gut microbiome.

1.5 Rationale and Research Objectives

Research has proven that xenobiotics, such as azo dyes, can be metabolized by the human gut microbiome. However, there is limited information concerning which species in the human gut microbiome can reduce azo bonds. There is even less information on the azoreductase enzyme found in obligate anaerobe species. These studies will illuminate which bacterial species are able to reduce azo bonds within a typical gut microbiome and the involvement of human azoreductase enzymes. It is important to understand the metabolism of food additives, especially those that are consumed in large amounts. As there is controversy over the impact of azo dyes on health, there is certainly a need for further research into food colourant azo dyes in order to determine how they are metabolized by the human gut microbiome. This will be explored through plate assay and enzyme activity-based processes.

The overall objectives of my research are to: (1) identify the prevalence of azo dye metabolism by the intestinal microbiota using an established strain library; (2) determine enzyme activity from identified strains with the four azo food dyes, Tartrazine, Sunset Yellow, Allura Red and Amaranth, (3) assess whether the presence of food azo dyes affects the growth of bacterial species, and (4) identify a putative azoreductase in a bacterial species which has the ability to reduce the dyes of interest.

2 Azo Dye Metabolism in the Gut Microbiome

2.1 Introduction

The toxicity and carcinogenicity of azo food dyes have been studied in *in vivo* models, focusing on dye ingestion in animals and *in vitro* tests for microbial dye reduction. Many azo dyes that when reduced produce toxic metabolites have been removed from use in food products; however, these dyes are still heavily prevalent in clothing production wastewater effluent[53]. These hazardous dyes are reduced by environmental microbes in the soil and water column[53,54]. There has thus been a recent focus on soil microbes azoreductase characterization with respect to carcinogenic dyes[53]. This research has been extended to azoreductase activity in human microbial communities, specifically to identify species with azo dye reduction capabilities. The classification of "azoreductase" properties in human gut microbiome species, regarding azo dyes found in food products, cannot be extrapolated from experiments performed with carcinogenic dyes (such as Orange I, Sudan I, Ponceau 3R etc.), which are not used in food products in the western world[1,10]. Species in the human gut microbiome encounter azo food dyes daily; chronic ingestion of one or more food azo dyes may cause shifts in human microbial communities, but this has yet to be determined.

In order to identify which bacterial species can reduce the four azo food dyes used in Canada, each substrate must be tested individually. Therefore, Amaranth, Allura Red, Sunset Yellow and Tartrazine were selected for testing against gut-derived bacterial isolates from several donors. Determining which species in a bacterial community can reduce a specific azo dye is an important step towards understanding the fate of these additives when they are ingested in foods. In this chapter, as well as determining which gut-derived bacterial species have food azo dye reductive capabilities, the growth of individual strains when exposed these four azo dyes is also investigated, in order to test whether some bacterial strains might be sensitive to the presence of either the compounds themselves or their metabolites.

2.2 Methods

2.2.1 Human Microbiome Strain Selection

Strains were selected from the strain collection the from Allen-Vercoe lab. The strain library used for this work consists of isolates of species from fecal samples of various donors. Isolates from two healthy donors (Donor 5 and Donor 6) were selected for initial azoreductase screening as representative of species in a healthy human gut microbiome. These strains were suspended in freezing media (Appendix 1) and were grown on Fastidious Anaerobic Agar (LabM) supplemented with 5% sheep's blood (Hemostat Laboratories) and incubated in an Anaerobe Systems anaerobic chamber at 37°C under an atmosphere of 10% CO_2, 10% H_2, and 80% N_2. After each strain selected for testing demonstrated growth on agar plates, a representative colony was selected and re-steaked. Following further incubation and growth, each strain's identity was confirmed by extracting crude DNA from subsample of biomass scraped from the plate, and using this as a template in PCR for 16S rRNA gene-based species identification as described in Section 2.1.2. Once isolates with azoreductase capabilities had been identified, different strains of the same species from other donors were selected from the Allen-Vercoe lab collection and tested.

2.2.2 16S rRNA Gene Sequence Analysis for Species Identification

Table 2.1 lists bacterial strains used in this thesis and their sources. Sanger sequencing was used to confirm the identities of the bacterial species from previously characterized communities; targets for Sanger sequencing were ~1kbp fragments of the 16S rRNA gene that were first amplified by PCR. Crude DNA was used as the template and a small (~1 µl) amount of biomass was added to an aliquoted PCR master mix which included: 10X Thermopol Reaction Buffer (Biolabs), 20 µM dNTP (Invitrogen), Taq polymerase (BioBasic), with 1 µl crude template DNA. The V3 region of the 16S rRNA gene was amplified using the primers V3kl (5N-

TACGG[AG]AGGCAGCA-3N) and V6r (5N-AC[AG]ACACGAGCTGACGAC-3N). The reaction conditions were 94°C for 2 min, (30s at 94°C, 30s at 60°C, 30s at 70°C) x 30 then 72°C for 5 min. The PCR products were confirmed by agarose gel electrophoresis with staining with Red Safe dye (iNtRON) after mixing with 1× loading dye (DyeNA-View) using a 1kb DNA molecular size ladder (Thermo Scientific) as a size guide. PCR products were then sent for Sanger sequencing at the Advanced Analysis Centre (University of Guelph) using BigDye Terminator v.3.1 (ThermoFisher) chemistry. Obtained sequences were BLASTed against the NCBI nucleotide database (https://www.ncbi.nlm.nih.gov/BLAST/) to infer identity.

2.2.3 Azoreductase Identification Plate Assay

For preliminary azoreductase testing, Fastidious anaerobic agar (FAA) plates (Neogen) were infused with 250 mg/L of 0.22 micron filter sterilized Amaranth, Allura Red, Sunset Yellow, Tartrazine or Evans Blue (Sigma). Dye plates were allowed to 'degas' (equilibrate with an anaerobic environment to ensure oxygen is displaced) in the anaerobe chamber for at least 1 hour before plating strains. Plates were divided into four, five, or six sections and 1µl of biomass was streaked as a lawn onto each section. Plates were incubated in the anaerobe chamber at 37°C for 72 h, and then removed for assessment, Tartrazine plates were exposed to air for 1 h and then images were taken of the plates. Results were plotted visually onto a phylogenetic tree that was created using a global alignment with a cost matrix of 93% similarity, and a Jukes-Cantor genetic distance model with neighbour-joining, by Geneious consensus phylogenetic tree building software Version 2020.03.

Table 2.1: Bacterial strains tested for azo dye reduction. Strains used in the whole bacterial cell azo dye kinetics and growth curve assays are indicated with "✓"

Source	Strain Name	Strain Code	Nearest Species ID	Percent ID	Kinetic/Growth Curve Assays Completed
Donor 5	22-5-I 11 TSAB	11 TSAB I	*Adlercreutzia equolifaciens*	100.0	
Donor 6	32-6-I 37 D6 FAA AN	37 D6 FAA I	*Agathobaculum butyriciproducens*	97.2	
Donor 5	22-5-S 18 FAA	18 FAA S	*Akkermansia muciniphila*	100.0	
Donor 5	22-5-S 5 D5 FAA	5 D5 FAA S	*Alistipes obesi*	100.0	
Donor 5	22-5-I 9 FAA NB	9 FAA NB I	*Alistipes onderdonkii*	100.0	
Donor 5	22-5-I 19 D5 FAA	19 D5 FAA I	*Alistipes putredinis*	100.0	
Donor 6	32-6-I 29 FAA AN	29 FAA I	*Alistipes putredinis*	100.0	
Donor 5	22-5-I 15 D5 FAA	15 D5 FAA I	*Alistipes shahii*	100.0	
Donor 6	32-6-I 16 MET AN	16 MET AN I	*Anaerostipes hadrus*	99.5	
Donor 6	32-6-I 6 D6 FAA AN	6 D6 FAA I	*Anaerostipes hadrus*	99.3	
Donor 6	16-6-I 7aii FAA	7aii FAA I	*Anaerostipes hadrus*	100.0	
Donor 6	32-6-I 19 NB AN	19 NB AN I	*Bacteroides caccae*	99.8	
Donor 6	32-6-I 30 NA AN	30 NA AN I	*Bacteroides caccae*	99.6	
Donor 5	22-5-I 12 FAA	12 FAA I	*Bacteroides cellulosilyticus*	99.8	
Donor 5	22-5-I 9 D5 FAA	9 D5 FAA I	*Bacteroides eggerthii*	100.0	
Donor 6	32-6-I 23 NB AN	23 NB AN I	*Bacteroides fragilis*	94.2	
Donor 6	32-6-S 4 D5 FAA AN	4 D5 FAA AN S	*Bacteroides fragilis*	98.6	
Donor 5	22-5-S 1 D6 FAA	1 D6 FAA S	*Bacteroides kribbi*	100.0	
Donor 5	22-5-S 16 BHI	16 BHI S	*Bacteroides kribbi*	100.0	
Donor 6	32-6-S 4 BHI AN	4 BHI AN S	*Bacteroides kribbi*	100.0	
Donor 6	32-6-I 3 D5 FAA AN	3 D5 FAA AN I	*Bacteroides kribbi*	100.0	
Donor 5	22-5-I 23 FAA	23 FAA I	*Bacteroides thetaiotaomicron*	100.0	
Donor 5	22-5-I 1 TSAB	1 TSAB I	*Bacteroides uniformis*	100.0	
Colon cancer biopsy	CC3/1 J4	CC3/1 J4	*Barnesiella intestinihominis*	99.1	✓
Colon cancer biopsy	CC2/1 M7	CC2/1 M7	*Barnesiella intestinihominis*	99.6	✓
Obese donor OB21	OB21 FMU 25	OB21 FMU 25	*Barnesiella intestinihominis*	98.9	✓
Donor 6	32-6-I 12 TSA AN	12 TSA AN I	*Bifidobacterium catenulatum*	100.0	
Donor 5	22-5-I 1 D6 FAA	1 D6 FAA I	*Bifidobacterium longum subsp. suillum*	100.0	
Donor 5	22-5-S 18 D6 FAA	18 D6 FAA S	*Blautia hydrogenotrophica*	99.8	
Donor 5	22-5-I 5 BHI	5 BHI I	*Blautia luti*	99.0	

Source	Strain Name	Strain Code	Nearest Species ID	Percent ID	Kinetic/Growth Curve Assays Completed
Donor 5	22-5-I 2 FAA NB	2 FAA NB I	*Blautia luti*	98.9	
Donor 5	22-5-S 4 TSA	4 TSA S	*Blautia producta*	100.0	
Donor 6	32-6-S 3 CNA AN	3 CNA AN S	*Blautia producta*	99.6	
Donor 5	22-5-S 1 D5 FAA AER	1 D5 FAA AER S	*Brevibacterium frigoritolerans*	100.0	
Donor 5	22-5-S 3 MRS	3 MRS S	*Catabacter hongkongensis*	100.0	
Donor 6	32-6-I 33 FAA AN	33 FAA AN I	*Clostridium glycyrrhizinilyticum*	100.0	
Donor 5	22-5-S 6 D6 FAA	6 D6 FAA S	*Clostridium hylemonae*	99.8	
Donor 5	22-5-S 8 D5 FAA	8 D5 FAA S	*Clostridium hylemonae*	97.8	
Donor 5	22-5-S 5 FAA	5 FAA S	*Clostridium innocuum*	98.7	✓
Donor 5	22-5-S 21 D6 FAA	21 D6 FAA S	*Clostridium pacaense*	99.7	✓
Donor 5	22-5-S 5 D6 FAA	5 D6 FAA S	*Clostridium scindens*	100.0	
Donor 6	32-6-S 9 CNA AN	9 CNA AN S	*Clostridium scindens*	99.3	
Donor 6	32-6-I 17 TSA AN	17 TSA AN I	*Clostridium spiroforme*	96.6	
Donor 6	32-6-I 7 MET AN	7 MET AN I	*Clostridium spiroforme*	94.0	
Donor 6	32-6-I 10 TSA AN	10 TSA AN I	*Clostridium spiroforme*	94.3	
Donor 5	22-5-S 2 FAA	2 FAA S	*Clostridium symbiosum*	98.3	✓
Colon cancer biopsy	CC33001A	CC33001A	*Clostridium symbiosum*	98.4	✓
Patient 54	7/3/54	7/3/54	*Clostridium symbiosum*	95.0	✓
Donor 5	22-5-I 6 FAA	6 FAA I	*Collinsella aerofaciens*	100.0	
Donor 5	22-5-I 20 D5 FAA	20 D5 FAA I	*Coprococcus catus*	96.2	
Donor 6	32-6-I 27 D6 FAA AN	27 D6 FAA AN I	*Coprococcus catus*	97.8	
Donor 5	22-5-I 1 BHI	1 BHI I	*Coprococcus comes*	100.0	
Donor 5	22-5-I 13 FAA	13 FAA I	*Coprococcus eutactus*	99.5	
Donor 5	22-5-S 2 BHI	2 BHI S	*Dielma fastidiosa*	99.5	✓
Donor 6	32-6-I 24 NB AN	24 NB AN I	*Dielma fastidiosa*	99.7	
Obese donor OB21	OB21 FMU 22 AN	OB21 FMU 22 AN	*Dielma fastidiosa*	98.3	
Donor 5	22-5-I 5 NA	5 NA I	*Dorea formicigenerans*	98.5	
Donor 6	32-6-S 1 FAA AN	1 FAA AN S	*Eggerthella lenta*	100.0	
Donor 6	32-6-S 25 D5 FAA AN	25 D5 FAA AN S	*Eggerthella lenta*	97.8	✓
Donor 5	22-5-S 13 D5 FAA	13 D5 FAA S	*Eisenbergiella tayi*	99.8	
Diabimmune T1D S	T1D S 5-17-FMU	17 FMU	*Enterocloster bolteae*	100.0	✓
Diabimmune T1D S	T1D S 2-1-GAM	1 GAM	*Enterocloster bolteae*	99.8	✓

Source	Strain Name	Strain Code	Nearest Species ID	Percent ID	Kinetic/Growth Curve Assays Completed
Diabimmune T1D NS	T1D NS 1-EtOH-30	EtOH30	*Enterocloster bolteae*	99.8	✓
Finegold	WAL 14578	WAL 14578	*Enterocloster bolteae*	100.0	
Ulcerative colitis patient 2	UC3-5-TSA	UC3 5 TSA	*Enterocloster bolteae*	100.0	
Donor 5	22-5-S 3 D6 FAA	3 D6 FAA S	*Enterocloster bolteae*	100.0	
Donor 5	22-5-S 11B D5 FAA	11B D5 FAA S	*Enterocloster lavalensis*	99.5	✓
Diabimmune T1D S	T1D S 5-32-GAM	32 GAM	*Enterocloster lavalensis*	100.0	
Donor 5	22-5-I 14 TSA	14 TSA I	*Erysipelatoclostridium ramosum*	100.0	
Donor 6	32-6-I 16 BHI AN	16 BHI AN I	*Erysipelatoclostridium ramosum*	100.0	
Donor 6	32-6-S 18 BHI AN	18 BHI AN S	*Escherichia fergusonii*	99.3	
Donor 5	22-5-S 11 NA	11 NA S	*Eubacterium callanderi*	99.8	
Donor 5	22-5-I 20 FAA	20 FAA I	*Eubacterium eligens*	100.0	
Donor 6	32-6-I 10 NA AN	10 NA AN I	*Eubacterium hallii*	98.0	
Donor 5	22-5-I 22 D6 FAA	22 D6 FAA I	*Eubacterium xylanophilum*	97.8	
Donor 6	32-6-I 30 D6 FAA AN	30 D6 FAA AN I	*Faecalicatena orotica*	96.8	
Donor 6	32-6-I 27 D5 FAA AN	27 D5 FAA AN I	*Flavonifractor plautii*	99.5	
Donor 5	22-5-I 24 FAA	24 FAA I	*Gemmiger formicilis*	99.3	
Donor 5	22-5-I 5 TSAB	5 TSAB I	*Holdemanella biformis*	97.8	
Donor 5	22-5-S 17 D6 FAA	17 D6 FAA S	*Holdemania massiliensis*	100.0	
Donor 6	32-6-S 5 D5 FAA AN	5 D5 FAA AN S	*Hungatella effluvii*	100.0	✓
Colon cancer biopsy	CC55-001-A	CC55001A	*Hungatella effluvii*	100.0	
Diabimmune T1D NS	T1D NS 0-9-FAA	9 FAA	*Hungatella effluvii*	98.4	
Diabimmune T1D NS	T1D NS 4-41-YPD	41 YPD	*Hungatella effluvii*	94.0	
Donor 5	22-5-S 17 D5 FAA	17 D5 FAA S	*Hungatella hathewayi*	97.8	
Diabimmune T1D S	T1D S 3-3-BHI	3 BHI	*Hungatella hathewayi*	100.0	✓
Donor 6	32-6-I 18 FAA AN	18 FAA AN I	*Lacrimispora amygdalinum*	97.0	
Donor 6	32-6-S 22 FAA AN	22 FAA AN S	*Lactonifactor longoviformis*	98.1	
Donor 5	22-5-S 17 FAA	17 FAA S	*Neglecta timonensis*	97.0	
Donor 5	22-5-S 3 FAA AER	3 FAA AER S	*Niallia circulans*	99.6	
Donor 5	22-5-I 21 D6 FAA	21 D6 FAA I	*Odoribacter splanchnicus*	100.0	✓
Donor 5	22-5-I 6 FAA NB	6 FAA NB I	*Oscillibacter ruminantium*	95.9	
Donor 6	32-6-S 11 BHI AN	11 BHI ANS	*Parabacteroides distasonis*	100.0	
Donor 5	22-5-I 16 FAA	16 FAA I	*Parabacteroides gordonii*	99.8	

Source	Strain Name	Strain Code	Nearest Species ID	Percent ID	Kinetic/Growth Curve Assays Completed
Donor 5	22-5-I 6 D6 FAA	6 D6 FAA I	*Parabacteroides merdae*	100.0	
Colon cancer biopsy	CC8-2-JVN-5b	CC8 2 JVN 5b	*Parasutterella excrementihominis*	99.4	
Donor 5	22-5-I 22 FAA	22 FAA I	*Phascolarctobacterium succinatutens*	99.7	
Donor 5	22-5-I 17 BHI	17 BHI I	*Phocaeicola vulgatus*	99.3	
Donor 6	32-6-I 1 D6 FAA AN	1 D6 FAA AN I	*Phocaeicola vulgatus*	98.9	
Donor 6	32-6-I 3 TSA AN	3 TSA AN I	*Phocaeicola vulgatus*	98.8	✓
Donor 5	22-5-I 5 D5 FAA	5 D5 FAA I	*Pseudoflavonifractor capillosus*	96.6	
Donor 5	22-5-S 12 D6 FAA	12 D6 FAA S	*Rarimicrobium hominis*	98.1	
Donor 5	22-5-I 10 D5 FAA	10 D5 FAA I	*Roseburia faecis*	99.8	
Donor 5	22-5-I 9A BHI	9A BHI I	*Roseburia hominis*	100.0	
Donor 5	22-5-S 6 FAA NB	6 FAA NB S	*Ruminococcus bromii*	98.9	
Donor 5	22-5-I 4 FAA	4 FAA I	*Ruminococcus faecis*	100.0	
Donor 6	32-6-I 21 NA AN	21 NA AN I	*Ruminococcus faecis*	97.2	
Donor 6	32-6-I 9 D6 FAA AN	9 D6 FAA AN I	*Ruminococcus gnavus*	99.4	
Donor 6	32-6-I 8 CNA AN	8 CNA AN I	*Ruminococcus gnavus*	99.3	
Donor 5	22-5-S 8 D6 FAA	8 D6 FAA S	*Ruminococcus torques*	97.9	
Donor 5	22-5-S 9B D6 FAA	9B D6 FAA S	*Ruminococcus torques*	99.1	
Donor 5	22-5-I 11 FAA	11 FAA I	*Ruminococcus torques*	99.2	
Donor 5	22-5-S 19 D5 FAA	19 D5 FAA S	*Ruthenibacterium lactatiformans*	99.4	
Donor 5	22-5-I 11 FAA NB	11 FAA NB I	*Sellimonas intestinalis*	100.0	
Donor 5	22-5-S 4 FAA AER	4 FAA AER S	*Staphylococcus epidermidis*	100.0	
Donor 5	22-5-S 1 FAA NB	1 FAA NB S	*Streptococcus periodonticum*	98.8	
Donor 5	22-5-S 11 FAA NB	11 FAA NB S	*Streptococcus salivarius*	100.0	
Donor 6	32-6-I 17 D6 FAA AN	17 D6 FAA AN I	*Sutterella stercoricanis*	97.0	
Donor 6	32-6-S 6 D5 FAA AN	6 D5 FAA NA S	*Sutterella stercoricanis*	97.2	
Donor 6	32-6-I 29 TSA AN	29 TSA NA I	*Veillonella atypica*	93.0	✓
Patient 44	3 1 44	3 1 44	*Veillonella atypica*	100.0	✓
Colon cancer biopsy	CC7/4 D6	CC7/4 D6	*Veillonella atypica*	96.5	
Diabimmune T1D S	T1D S 2-5-FAA-AN	5 FAA AN	*Veillonella atypica*	100.0	
Non-NEC infant fecal sample	NND8-Rd4-V2-8-TSA-AN	Rd4 V2 8 TSA AN	*Veillonella atypica*	100.0	
Colon cancer biopsy	CC7/4 MRS 1	CC7/4 MRS 1	*Veillonella dispar*	99.5	
Colon cancer biopsy	CC3/3 JVN 5	CC3/3 JVN 5	*Veillonella dispar*	98.8	

Source	Strain Name	Strain Code	Nearest Species ID	Percent ID	Kinetic/Growth Curve Assays Completed
Colon cancer biopsy	CC7/4 NA 2	CC7/4 NA 2	*Veillonella dispar*	99.0	
Donor 6	32-6-I 27 FAA AN	27 FAA AN I	*Veillonella dispar*	99.7	
Colon cancer biopsy	CC1/6 J4	CC1/6 J4	*Veillonella dispar*	100.0	
Diabimmune T1D_NS	T1D_NS_4-23-PEC-AN	23 PEC AN	*Veillonella dispar*	100.0	
Non-NEC infant fecal sample	NND8-Rd1-V3-1-TSA-AN	Rd1 V3 1 TSA AN	*Veillonella dispar*	99.7	
Finegold strain	WAL 16971	WAL 16971	*Veillonella dispar*	100.0	
Obese donor OBEAV1	OBEAV1 6 MRS	OBEAV1 6 MRS	*Veillonella dispar*	99.6	✓
Patient 27	6_1_27	6_1_27	*Veillonella parvula*	99.0	✓
Patient with PANDAS	AC2811 AN NA 2	AC2811	*Veillonella parvula*	99.6	

Source – The donor that the strain was isolated from

Strain Name – The name assigned to the strains at the time of isolation

Strain Code – The code assigned for strain in this thesis

Nearest Species ID – The result of a BLASTn search of approximately 600-800bp of 16S rRNA gene sequence generated using the Sanger method on extracted gDNA from each strain

Kinetic/Growth Curve Assays Completed – Strains used in kinetic and growth curve assays

2.2.4 Whole Bacterial Cell Azo Dye Kinetics

All reagents were allowed to degas in the anaerobe chamber for 24 h before plate assays were performed. Strains of interest were grown in 0.22 micron filter sterilized Brain Heart Infusion (BHI) broth (Difco) in sterile glass test tubes at 37°C in the anaerobic chamber with the atmosphere: 10% CO_2, 10% H_2, 80% N_2. Strains were inoculated into media by scraping a 1µg loopful of biomass from a freshly grown plate. Strains were grown at 37°C until they reached an OD600 >0.05. All strains were standardized in BHI medium to OD600 = 0.05 (with exception of the *Dielma fastidiosa* strain which was grown and standardized to OD600 = 0.02). Azo dyes (Amaranth, Allura Red, Sunset Yellow or Tartrazine) were added to BHI broth to final concentration = 250 µM and then 0.22 micron filter sterilized. The strains were screened using polystyrene 96-well plates (Falcon); standardized strains were inoculated into the filter sterilized dye medium at 1/100 dilution; final volume 200 µl. The wells were covered with 50 µl of 0.22

micron filter sterilized mineral oil (Sigma), then incubated in a Biotek Epoch 2 plate reader set at 37°C, housed in a Baker Concept anaerobe chamber under an atmosphere of 10% CO_2, 10% H_2, 80% N_2. Measurements were taken over a 24 h period at the peak wavelength for each dye (Amaranth: 521 nm, Allura Red: 406 nm, Sunset Yellow: 481 nm, Tartrazine: 427 nm) every 30 min. All strains tested are listed in Table 2.1. Kinetics plots were drawn with Prism 9 (GraphPad).

Four technical replicates were completed for each strain and the standard deviation of the mean was calculated. Outliers were detected and removed using the ROUT test with Q = 1%. The statistical significance of reduction was calculated using paired t-test in Prism 9 (GraphPad) and was determined to be ($P>0.05$). A negative control of BHI medium without strains or azo dyes added was included on each plate to establish the baseline absorbance of the media. A positive control of BHI supplemented with azo dye (Amaranth, Allura Red, Sunset Yellow, Tartrazine) was included to establish the baseline absorbances of the dye media.

2.2.5 Growth Curve Assay

For conducting growth curve assays, the same protocol was used as in section 2.1.4, except that wavelength 600 nm was employed, and data points were collected every 15 min. This assay was completed for dyes Sunset Yellow and Tartrazine at final concentration 250 μM. The presence of dyes Allura Red and Amaranth at 250 μM interfered with the readings for growth at OD600 and therefore, for these dyes, growth curves were not carried out. For strain growth analysis the same protocol was conducted as in section 2.1.4, apart from measuring the growth of the strains at 600 nm. A negative control of BHI media without strains or azo dyes added was included on each plate to ensure media sterility. A positive control of BHI supplemented with either Tartrazine or Sunset Yellow was included to establish the baseline absorbances of the dye media.

2.3 Results

2.3.1 Azo Dye Reduction Plate Assay

In order to understand the extent of azo dye reduction capability among diverse gut microbiota strains, a screening plate assay was utilized. In this test, azo dyes were infused into a broadly supportive agar medium and colonies of tested strains were allowed to grow on this medium. A positive result for the azo dye reduction agar plate assay was classified as a section of an azo dye-containing plate where growth of a given isolate correlated with visual decolourization, indicating that a species was positive for azo dye reduction. Figure 2.1 demonstrates this phenomenon using five azo dye infused plates, including Amaranth, Allura Red, Sunset Yellow, Tartrazine and Evans Blue. The sections of the agar plate that show azo dye reduction correlate with *Veillonella* sp. strains CC7/4 MRS 1, AC2811, and 6_1_27. One section with no decolourization is associated with growth of *Parasutterella* sp. strain CC8/2 JVN 5b, whereas the final section with no decolorization is an inoculated control. The *Veillonella* spp. were able to reduce all five azo dyes tested within a 72 h incubation period, and were selected for further study. Figure 2.1.1 shows the formation of a purple product in an aerobic environment following the anaerobic reduction of Tartrazine.

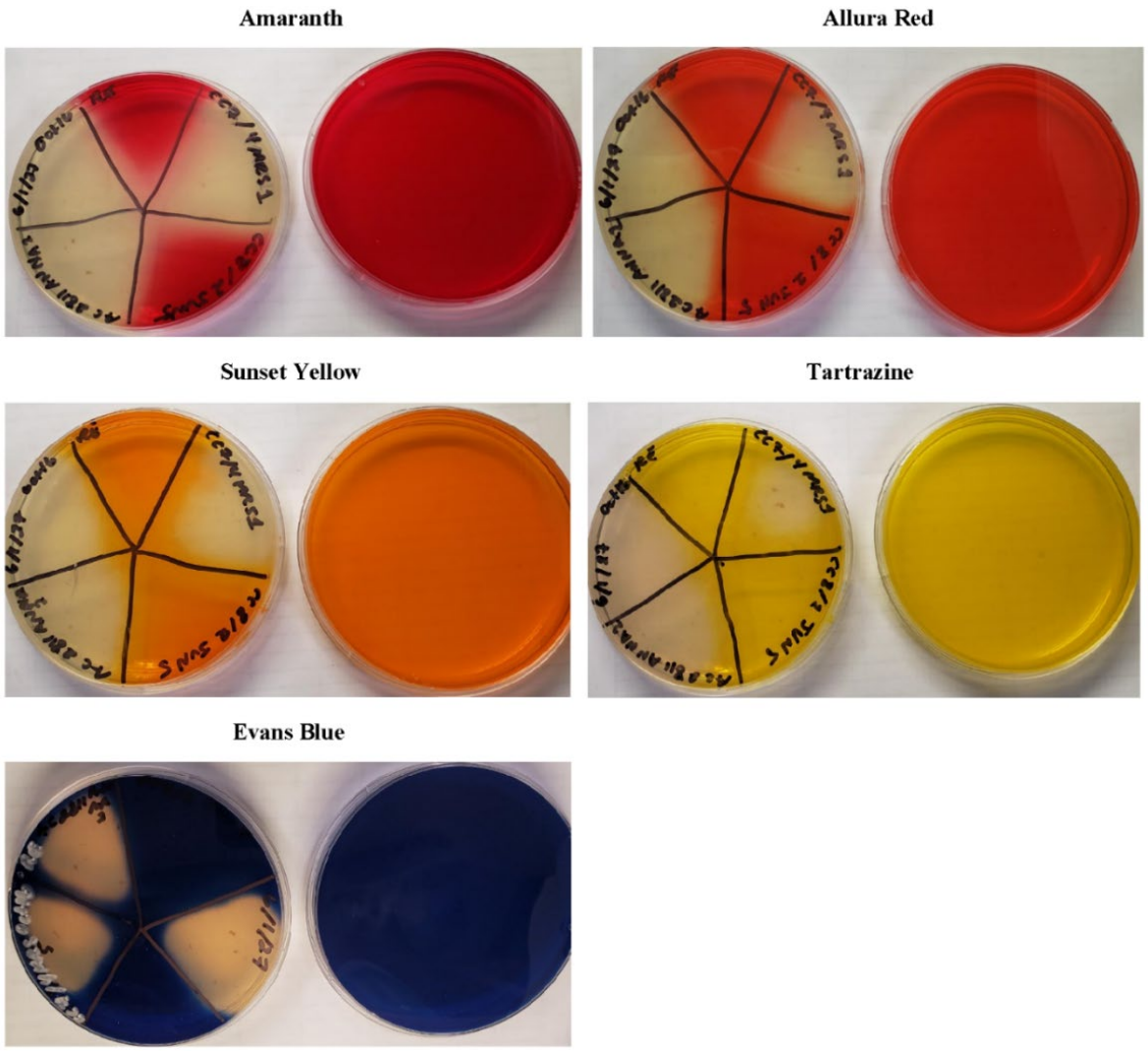

Figure 2.1: Azo dye-containing FAA plates after 72 h incubation at 37°C under anaerobic conditions with strains of interest. Plates were divided into 4, 5 or 6 sections, and inoculation of a given strain was restricted to a relevant section. Plates on the left have sections with bacterial growth and show sections with azo dye reduction (decolourization). The plates on the right are control plates with no bacteria.

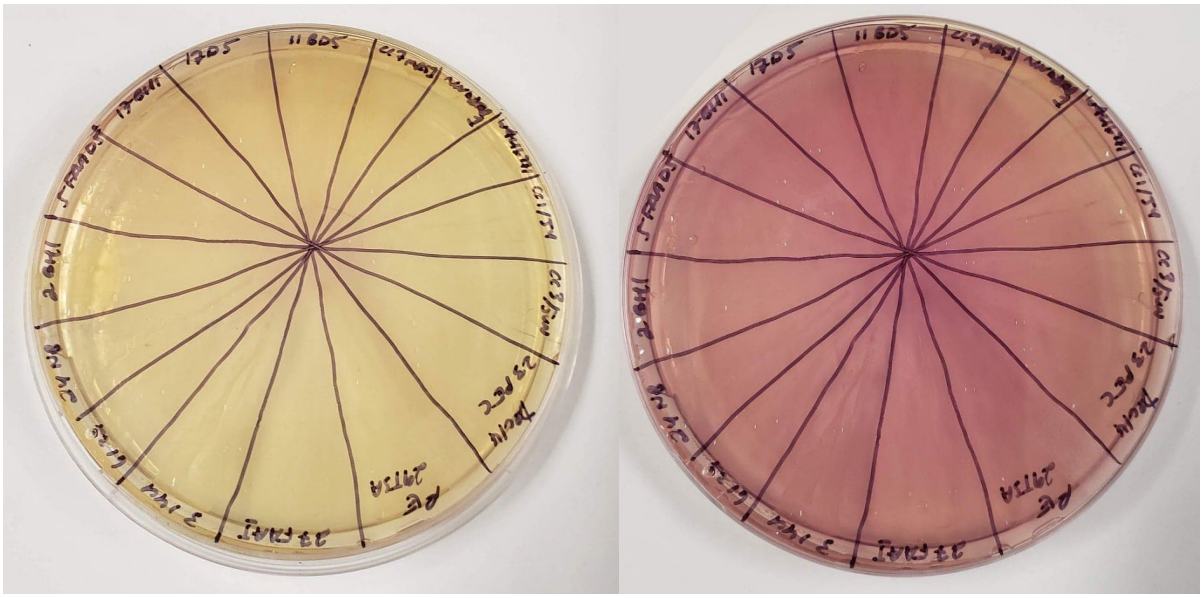

Figure 2.1.1: The image on the left shows a decolourized FAA plate containing Tartrazine after 72 h incubation at 37°C under anaerobic conditions with strains of interest. The plate was divided into 16 sections, and inoculation of a given strain was restricted to a relevant section. The image on the left shows complete Tartrazine reduction after 72 h of growth. The image on the right shows the colour change when the plate was exposed to air for 1 h.

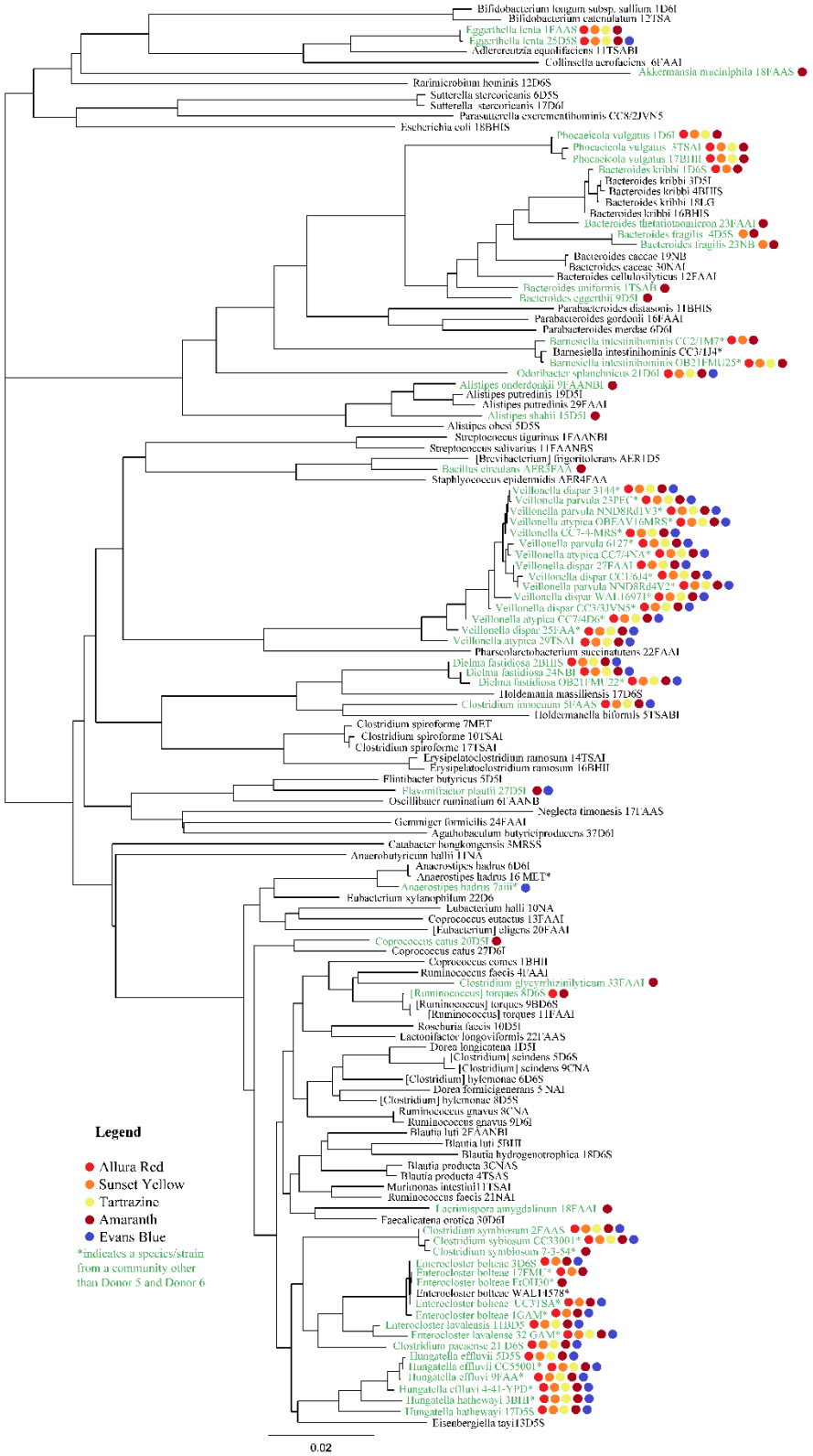
Bifidobacterium longum subsp. suillum 1D6I
Bifidobacterium catenulatum 12TSA
Eggerthella lenta 1FAAS
Eggerthella lenta 25D5S
Adlercreutzia equolifaciens 1TSABI
Collinsella aerofaciens 6I7AAI
Akkermansia muciniphila 18FAAS
Rarimicrobium hominis 12D6S
Sutterella stercoricanis 6D5S
Sutterella stercoricanis 17D6I
Parasutterella excrementihominis CC8/2JVN5
Escherichia coli 18BHIS
Phocaeicola vulgatus 1D6I
Phocaeicola vulgatus 3TSAI
Phocaeicola vulgatus 17BHIE
Bacteroides kribbi 1D6S
Bacteroides kribbi 3D5I
Bacteroides kribbi 4BTTS
Bacteroides kribbi 18LG
Bacteroides kribbi 16BHIS
Bacteroides thetatiotaomicron 23FAAI
Bacteroides fragilis 4D5S
Bacteroides fragilis 23NB
Bacteroides caccae 19NB
Bacteroides caccae 30NAI
Bacteroides cellulosilyticus 12FAAI
Bacteroides uniformis 1TSAB
Bacteroides eggerthii 9D5I
Parabacteroides distasonis 11BHIS
Parabacteroides gordonii 16FAAI
Parabacteroides merdae 6D6I
Barnesiella intestinihominis CC2/1M7*
Barnesiella intestinihominis CC3/1J4*
Barnesiella intestinihominis OB21FMU25*
Odoribacter splanchnicus 21D6I
Alistipes onderdonkii 9FAANBI
Alistipes putredinis 19D5I
Alistipes putredinis 29FAAI
Alistipes shahii 15D5I
Alistipes obesi 5D5S
Streptococcus tigurinus 1FAANBI
Streptococcus salivarius 11FAAN8S
[Brevibacterium] frigoritolerans AER1D5
Bacillus circulans AER3FAA
Staphylococcus epidermidis AER4FAA
Veillonella dispar 3144*
Veillonella parvula 23PEC*
Veillonella parvula NND8Rd1V3*
Veillonella atypica OBFAV16MRS*
Veillonella CC7-4-MRS*
Veillonella parvula 6127*
Veillonella atypica CC7/4NA*
Veillonella dispar 27FAAI
Veillonella dispar CC1/61d*
Veillonella parvula NND8Rd4V2*
Veillonella dispar WAL16971*
Veillonella dispar CC3/3JVN5*
Veillonella atypica CC7/4D6*
Veillonella dispar 25FAA*
Veillonella atypica 29TSAI
Pharseolactobacterium succinatutens 22FAAI
Dielma fastidiosa 2IBIIS
Dielma fastidiosa 24NBI
Dielma fastidiosa OB21FMU22*
Holdemania massiliensis 17D6S
Clostridium innocuum 5IFAAS
Holdemanella biformis 5TSABI
Clostridium spiroforme 7MET
Clostridium spiroforme 10TSAI
Clostridium spiroforme 17TSAI
Erysipelatoclostridium ramosum 14TSAI
Erysipelatoclostridium ramosum 16BHII
Flintibacter butyricus 5D5I
Flavonifractor plautii 27D5I
Oscillibacter ruminatium 6I7AANB
Neglecta timonesis 17TAAS
Gemmiger formicilis 24FAAI
Agathobaculum butyriciproducens 37D6I
Catabacter hongkongensis 3MRSS
Anaerobutyricum hallii 1TNA
Anaerostipes hadrus 6D6I
Anaerostipes hadrus 16 MET*
Anaerostipes hadrus 7aii*
Rubacterium xylanophilum 22D6
Lubacterium halli 10NA
Coprococcus eutactus 13FAAI
[Eubacterium] eligens 20FAAI
Coprococcus catus 20D5I
Coprococcus catus 27D6I
Coprococcus comes 1BHII
Ruminococcus faecis 4I7AAI
Clostridium glycyrrhizinilyticum 33FAAI
[Ruminococcus] torques 8D6S
[Ruminococcus] torques 9BD6S
[Ruminococcus] torques 11FAAI
Roseburia faecis 10D5I
Lactonifactor longoviformis 22I7AAS
Dorea longicatena 1D5I
[Clostridium] scindens 5D6S
[Clostridium] scindens 9CNA
[Clostridium] hylemonae 6D6S
Dorea formicigenerans 5 NAI
[Clostridium] hylemonae 8D5S
Ruminococcus gnavus 8CNA
Ruminococcus gnavus 9D6I
Blautia luti 2FAANBI
Blautia luti 5BHI
Blautia hydrogenotrophica 18D6S
Blautia producta 3CNAS
Blautia producta 4TSAS
Murimonas intestinii11TSAI
Ruminococcus faecis 21NAI
Lacrimispora amygdalinum 18FAAI
Faecalicatena orotica 30D6I
Clostridium symbiosum 2FAAS
Clostridium sybiosum CC33001*
Clostridium symbiosum 7-3-54*
Enterocloster bolteae 3D6S
Enterocloster bolteae 17FMU*
Enterocloster bolteae EtOH30*
Enterocloster bolteae WAL11578*
Enterocloster bolteae UCYISA*
Enterocloster bolteae 1GAM*
Enterocloster lavalensis 11BD5
Enterocloster lavalense 32 GAM*
Clostridium pacaense 21 D6S
Hungatella effluvii 5D5S
Hungatella effluvii CC55001*
Hungatella effluvii 9FAA*
Hungatella effluvi 4-41-YPD*
Hungatella hathewayi 3BIII*
Hungatella hathewayi 17D5S
Eisenbergiella tayi13D5S
Legend
Allura Red
Sunset Yellow
Tartrazine
Amaranth
Evans Blue
*indicates a species/strain from a community other than Donor 5 and Donor 6
0.02

Figure 2.2: Phylogenetic map constructed using 16S rRNA gene sequences to determine relatedness of over 130 tested isolates representing six phyla, derived from fecal microbiomes. Where possible, isolates related to strains that initially showed azo dye decolorization activity were selected from the Allen-Vercoe lab collection for testing to assess broad activity among a species or clade. Names of bacterial strains that reduced azo dyes are coloured green. The ability to reduce azo dyes was determined from the assay shown in Figure 2.1.

The data collected from the azo dye plate assay (Table 2.1 and Figure 2.2) demonstrates that the azo dye most frequently reduced by gut microbiome-associated species was Amaranth, and the least frequently reduced was Tartrazine. Sunset Yellow, Evans Blue and Allura Red were the second, third and fourth most reduced dyes, respectively. Evans Blue was used as an indicator substrate since the dark blue colour contrasted well against the slight yellow colour of the agar plates when reduced, whereas the reduction of Tartrazine was not as distinct visually (Figure 2.1). It was thus theorized that Evans Blue could be used as an indicator dye to identify whether a strain has azoreductase capabilities. However, it was not reduced as frequently as Amaranth in the assays performed here. Therefore, Amaranth was determined to be the best identifier of whether a strain has azoreductase capabilities (Table 2.1).

The reduction of these five azo dyes was not always consistent among strains of the same species, for example, strains associated with species *Ruminococcus torques, Coprococcus catus, Enterocloster bolteae, Anaerostipes hadrus, Bacteroides kribbi, Barnesiella intestinihominis,* and *Clostridium symbiosum* were not all able to produce areas of decolorization on plates. Taxa exhibiting high azo dye reduction activity in this survey belonged to the genera *Clostridium, Hungatella, Enterocloster, Veillonella, Dielma, Eggerthella, Odoribacter*, and *Phocaeicola.*

The phylogenetic mapping of all the species screened for azoreductase capabilities (Figure 2.2) shows the genetic similarities between species with high azoreductase activity. Species that showed some azo dye reduction activities were not all closely related, but instead spread across the tree. However, there were clusters of species that reduced many azo dyes. Three clusters in particular fell into this category: the first included *Clostridium symbiosum,*

Clostridium pacaense, Enterocloster bolteae, Enterocloster lavalensis, Hungatella effluvii and Hungatella hathewayi, all of which belong to the family Lachnospiraceae, a prominent group within the human gut microbiome[55]. The second cluster included members of the Veillonella genus: *Veillonella atypica, Veillonella parvula* and *Veillonella dispar,* as well as representative isolates of *Dielma fastidiosa* and *Clostridium innocuum* species, belonging to the *Erysipelotrichales* order[56]. The third cluster included strains associating with *Phocaeicola vulgatus, Barnesiella intestinihominis,* and *Odoribacter splanchnicus* species, which are all members of the *Bacteroidales* order[56]. Representative strains of *Eggerthella lenta*, a member of the Eggerthellaceae group of the Actinobacteria phyla, also showed abilities to broadly reduce the tested azo dyes. One strain of *Akkermansia muciniphila,* a Verrucomicrobia phylum member, was tested in this assay, and found to reduce Amaranth.

2.3.2 Whole Bacterial Cell Azo Dye Kinetics

A quantitative method to measure azo dye reduction was achieved by observing dye reduction over a physiologically relevant time period, as 24 hours is the average retention time in the human colon [57]. To do this, a plate reader assay was employed to measure absorbance at the appropriate wavelength for each dye during growth of selected strains over time. Data was presented according to the species' genetic similarities, and general patterns of reduction shown. The positive control is BHI medium with azo dye present which represents the maximum absorbance of the dye at full saturation and the negative control is just the BHI medium (absorbance with no azo dye present).

The findings of the azoreductase agar plate assay corroborate the results of the 96-well whole bacterial cell azo dye kinetics. Overall, Amaranth was the most, and Tartrazine the least frequently reduced substrate. As seen in section 2.2.2, there was a difference in the reduction of the four azo dyes between strains of the same species. This was exemplified by strains of the species *C. symbiosum, E. bolteae,* and *B. intestinihominis*.

The *C. symbiosum,* strains 2 FAA S and CC33001A showed reduction of all four azo food dyes, whereas strain 7/3/54 only showed very slight reduction of Amaranth (Figure 2.3). The strains CC33001A and 2 FAA S showed similar dye reduction for all four of the azo dyes tested. There was no difference in reduction activity or rate between Amaranth and Allura Red substrates for these strains; for both, there was complete reduction before 10 hours of incubation. There was a delay in the complete reduction time for Sunset Yellow, with complete reduction for these strains by about 20 hours of incubation. Tartrazine was the only dye that was not completely reduced by these strains during the 24 h incubation time.

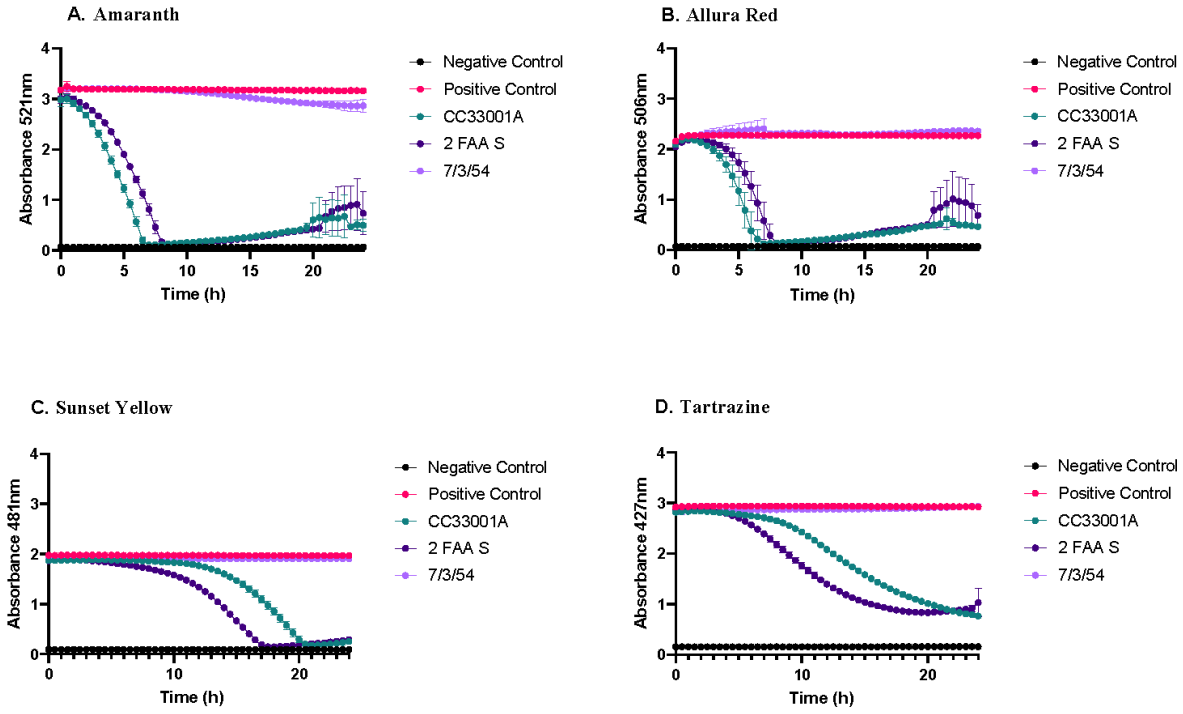

Figure 2.3: The 24 h incubation of *C. symbiosum* strains CC33001A, 2 FAA S, and 7/3/54, at 37°C under anaerobic conditions. The reduction of 250 µM azo dye was measured at the peak wavelength for A. Amaranth, B. Allura Red, C. Sunset Yellow, and D. Tartrazine.

The reduction patterns of the *C. symbiosum* strains were reflected in the *E. bolteae* strains, where there were differences in dye reduction between strains of the same species. Over the 24 h assay, the *E. bolteae* strains 17 FMU and 1 GAM showed comparable reduction patterns with all four azo dyes, with Amaranth and Allura Red being fully reduced in the 24 h period. Sunset Yellow had slight reduction while reduction of Tartrazine was not observed (Figure 2.4). Strain EtOH30 only showed slight reduction of Amaranth, and no reduction for the other three azo dyes within the incubation period. This validates the plate assay results in Section 2.2.1 where *E. bolteae* species did not reduce Tartrazine and the only dye strain EtOH30 reduced was Amaranth.

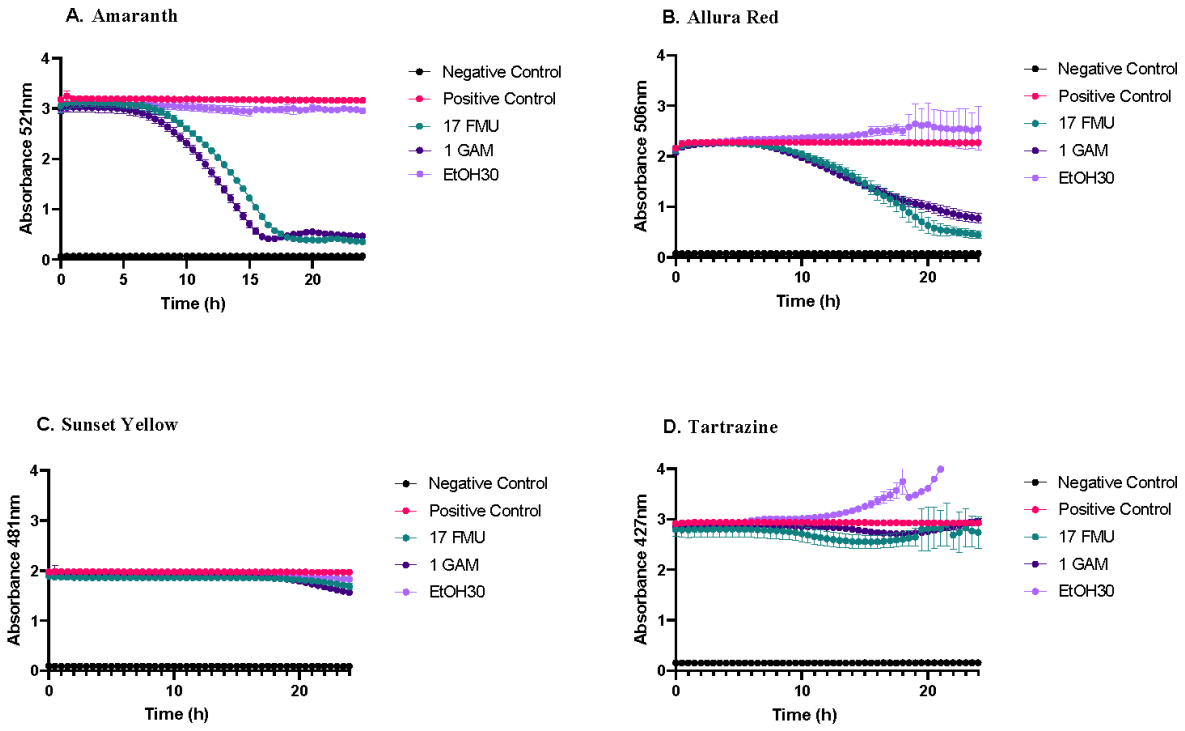

Figure 2.4: The 24 h incubation of *E. bolteae* strains 17 FMU, 1 GAM, and EtOH30, at 37°C under anaerobic conditions. The reduction of 250 µM azo dye was measured at the peak wavelength for A. Amaranth, B. Allura Red, C. Sunset Yellow, and D. Tartrazine.

The *Veillonella* spp. all showed a very rapid reduction of Amaranth as evident from the complete reduction of the dye before the incubation period. Tartrazine was slightly reduced by strain 29 TSA during the 24 h incubation (Figure 2.5). All strains of this genus have very similar dye reduction patterns; however, strains 29 TSA and OBEAV1 6 MRS, which are both *V. atypica*, showed the most variance. These results do not reflect the data shown in the plate assay, Section 2.2.1.

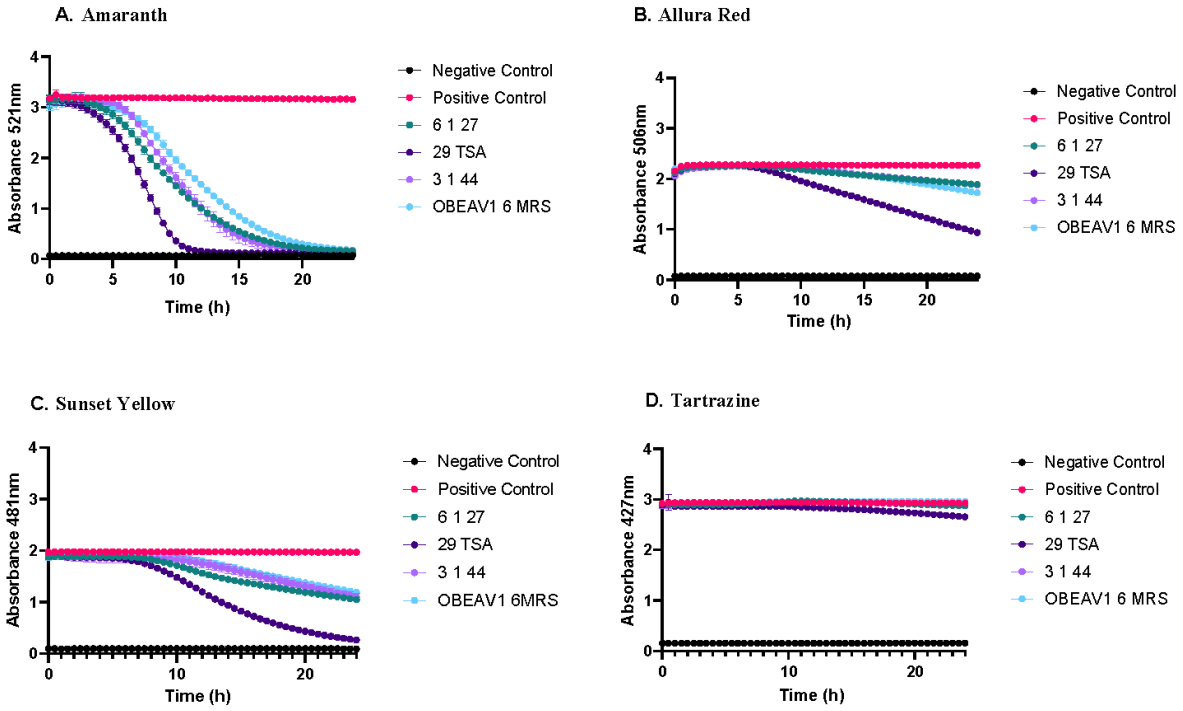

Figure 2.5: The 24 h incubation of *V. parvula* strain 6_1_27, *V. atypica* strains 29 TSA, and OBEAV1 6 MRS, and *V. dispar* strain 3_1_44, at 37°C under anaerobic conditions. The reduction of 250 µM azo dye was measured at the peak wavelength for A. Amaranth, B. Allura Red, C. Sunset Yellow, and D. Tartrazine.

The Bacteroidota strains 3 TSA, CC3/1 J4 and CC2/1 M7, and 21 D6 I did not show reduction of any of the four food azo dyes over the 24 h test period (Figure 2.6); the only strain

of *B. intestinihominis* that demonstrated azo dye reduction was OB21 FMU 25. This strain reduced Allura Red and Amaranth to completion, within the 24 h incubation period, with Allura Red being reduced in less time. The same strain also reduced Sunset Yellow and Tartrazine, but neither dye was reduced to completion within 24 h. The rate of reduction of Tartrazine appeared to be slower overall but with earlier onset than that of Sunset Yellow (Figure 2.6).

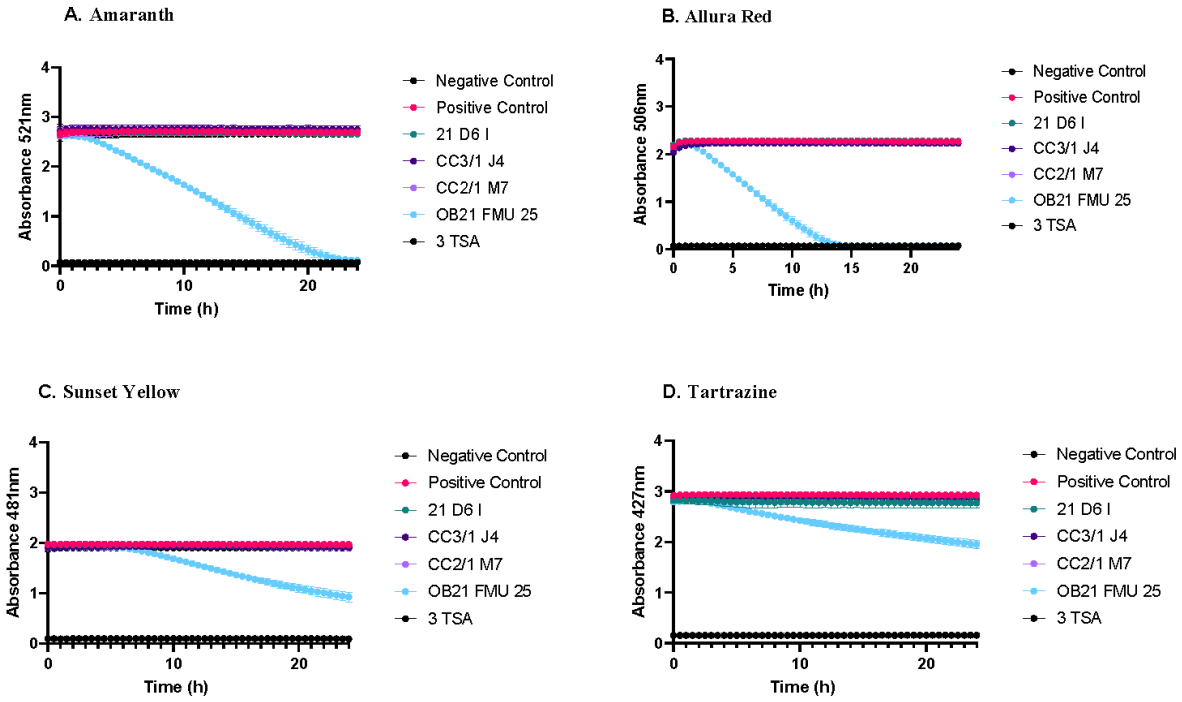

Figure 2.6: The 24 h incubation of *O. splanchnicus* strain 21 D6 I, *B. intestinihominis* strains CC3/1 J4, CC2/1 M7 AND OB21 FMU 25, and *P. vulgatus* strain 3 TSA, at 37°C under anaerobic conditions. The reduction of 250 µM azo dye was measured at the peak wavelength for A. Amaranth, B. Allura Red, C. Sunset Yellow, and D. Tartrazine.

Strains 3BHI, 21 D6 S, 5 FAA S, 11 B D5, 2 BHI and 25 D5 S, representative of various species across several phyla, were able to reduce all four of the azo dyes within 24 h, with Amaranth reduction at the fastest rate, and Tartrazine at the slowest rate (Figure 2.7). Strains 25

D5 S and 5 FAA S had the shortest complete azo dye reduction times. The strain 2 BHI had the most linear reduction pattern for all four azo dyes. These results matched the reduction data from the plate assay in section 2.2.2.

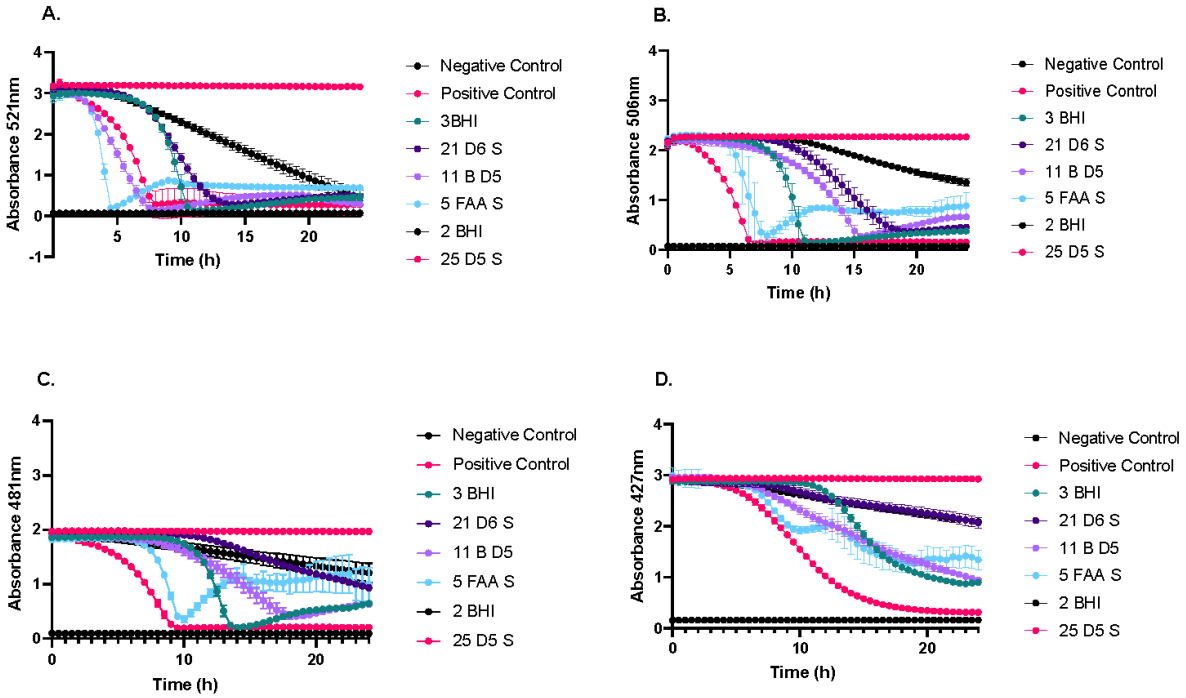

Figure 2.7: The 24 h incubation of *H. effluvii* strain 3 BHI, *C. pacaense* strain 21 D6 S, *E. lavalensis* strain 11 B D5, *C. innocuum* strain 5 FAA, *D. fastidiosa* strain 2 BHI, and *E. lenta* strain 25 D5 S, at 37°C under anaerobic conditions. The reduction of 250 µM azo dye was measured at the peak wavelength for A. Amaranth, B. Allura Red, C. Sunset Yellow, and D. Tartrazine.

2.3.3 Growth Curve Kinetics

Next, it was important to determine whether growth of each isolate took place during the reduction assays outlined in Section 2.2.2. The results for the tested strains are presented here in the same grouping as in Section 2.2.2, except for *D. fastidiosa* strain 2 BHI and *E. lenta* strain 25 D5 S, which were grouped with *Veillonella* spp. to allow a better visualization of growth

patterns; this growth curve was included as an example, with all other growth curves included in Appendix 2. The positive controls for both Tartrazine and Sunset Yellow displayed no additional interference at 600 nm compared to the negative medium control, whereas Amaranth and Allura Red had a high absorbance and interference at 600 nm. The error bars represent the average of four technical replicates of each data point.

The strains that showed no discernible growth in any medium type were the *Barnesiella* spp. strains CC3/1 J4, CC2/1 M7, *Dielma* sp. strain 2 BHI, and *Phocaeicola sp.* strain 3 TSA (Figure 2.8 and Appendix 2, Figure D); with exception to 2 BHI, this suggests that the lack of azo dye reduction by these species could be caused by a lack of growth. The species 2 BHI does not show growth in any medium type; however, it was able to reduce all four azo dyes. The *Barnesiella sp.* strain OB21 FMU 25 showed marginal growth in Sunset Yellow-infused media and BHI media (Appendix 2, Figure D) this was the only strain to grow and the only strain to show azo dye reduction. The *Odoribacter* sp. strain 21 D6 I showed slight growth in the BHI medium only and inhibited growth in the azo dye-supplemented media (Appendix 2, Figure D). The growth of the multiple *Veillonella* spp. strains tested and *Eggerthella* strain 25 D5 S did not seem to be affected greatly by the azo dye supplemented media. (Figure 2.8).

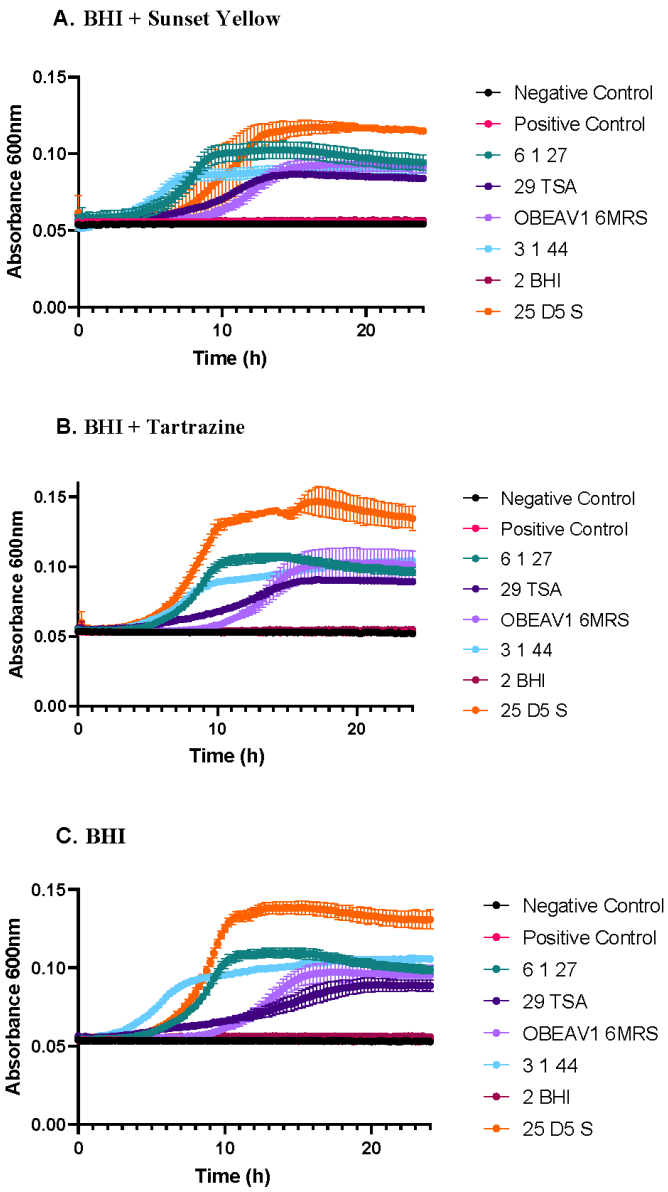

Figure 2.8: The 24 h incubation of *V. parvula* strain 6_1_27, *V. atypica* strains 29 TSA, and OBEAV1 6 MRS, *V. dispar* strain 3_1_44, *D. fastidiosa* 2 BHI, and *E. lenta* 25 D5 S at 37°C under anaerobic conditions. The growth of these strains was measured in BHI or BHI media supplemented with 250 µM azo dye.

All the *E. bolteae* strains tested showed suppressed growth in Sunset Yellow supplemented media, and very minimal growth in Tartrazine supplemented media compared to control (Appendix 2, Figure B). This growth aligns with the results from kinetics with whole cell bacterial preparations, which demonstrated that these strains did not reduce Tartrazine (Figure 2.4) and corroborates the agar plate assay (Table 2.). Similarly, the *C. symbiosum* strains 7/3/54, 2 FAA S and CC33001A displayed delayed growth in medium supplemented with azo dyes compared to controls (Appendix 2, Figure A). Strain 7/3/54 has the slowest growth out of all the *C. symbiosum* strains, and strain EtOH30 had the slowest growth out of all the *E. bolteae* strains, and in all media types (Figure 2.3 and 2.4). The limited growth of these strains may affect their ability to reduce the azo dyes. In Sunset Yellow medium there was inhibited growth of *C. symbiosum* strain 5 FAA S when compared to growth in BHI and Tartrazine. However, this was difficult to compare since the replicate error increased after 10 hours of growth. The same strain grown in the presence of Tartrazine showed increased growth vs. BHI (Appendix 2, Figure C). The growth of *O. splanchnicus* strain 21 D6 S was both delayed and suppressed in Tartrazine and Sunset Yellow compared to the control media (Appendix 2, Figure C). The growth of *H. effluvii* strain 3 BHI and *C. lavalensis* 11 B D5 was similar between all medium types (Appendix 2, Figure C).

2.4 Discussion

It is known that azo reductases are present in some bacteria and catalyze the reduction of azo dyes. However, it has not been confirmed that these enzymes are present in commensal gut bacteria, and there may be different mechanisms for azo dye reduction among bacterial species. Alternatively, if gut commensal bacterial species share similar azoreductase enzymes, then the mechanism of binding of the azo dye substrate could be the factor responsible for the differences in substrate reduction rates seen. The four azo food dyes tested in this work have some similarities in structure and are sulphonated; however, Amaranth is the only dye that has two

fused aromatic six membered rings on either side of the azo bond (Figure 1.5). This unique attribute of Amaranth structure could thus contribute to its frequent and rapid susceptibility to reduction compared to the other tested dyes; for example, there may be specificity in the reduction of azo dyes if the azo reduction is caused by azoreductase enzymes with active sites that favor the structure of Amaranth compared to the other dyes. The structures of Allura Red and Sunset Yellow both form 1-amino-2-naphthol-6-sulphonic acid after azo bond reduction (Figure 2.9), which correlates to the similar reduction of both of these dyes (section 2.2.2). From this work, a relationship has emerged between the structure of a given azo dye and the ability of commensal gut bacterial species to reduce them. One of the only azo dyes that contains a five membered ring is Tartrazine, and it is possible that this structure contributed to the apparent difference in reduction ability and kinetics of this dye compared to the other three azo dyes. Further work to identify potential azoreductases and to obtain crystal structures will be required in order to fully characterize their binding domains, and to determine enzyme substrates.

The formation of the purple product after the aerobic incubation of reduced Tartrazine metabolites (Figure 2.1.1) reflects what has been seen previously by Perez-Diaz *et al*. in broth culture, and Westöö in rats [30,31]. This establishes that this product can be produced in agar when Tartrazine is reduced by individual bacterial species. The structure of the product was not identified. In future experiments, this purple product could be isolated and identified via LC-MS to confirm the molecular weight in relation to Westöö's predicted metabolite.

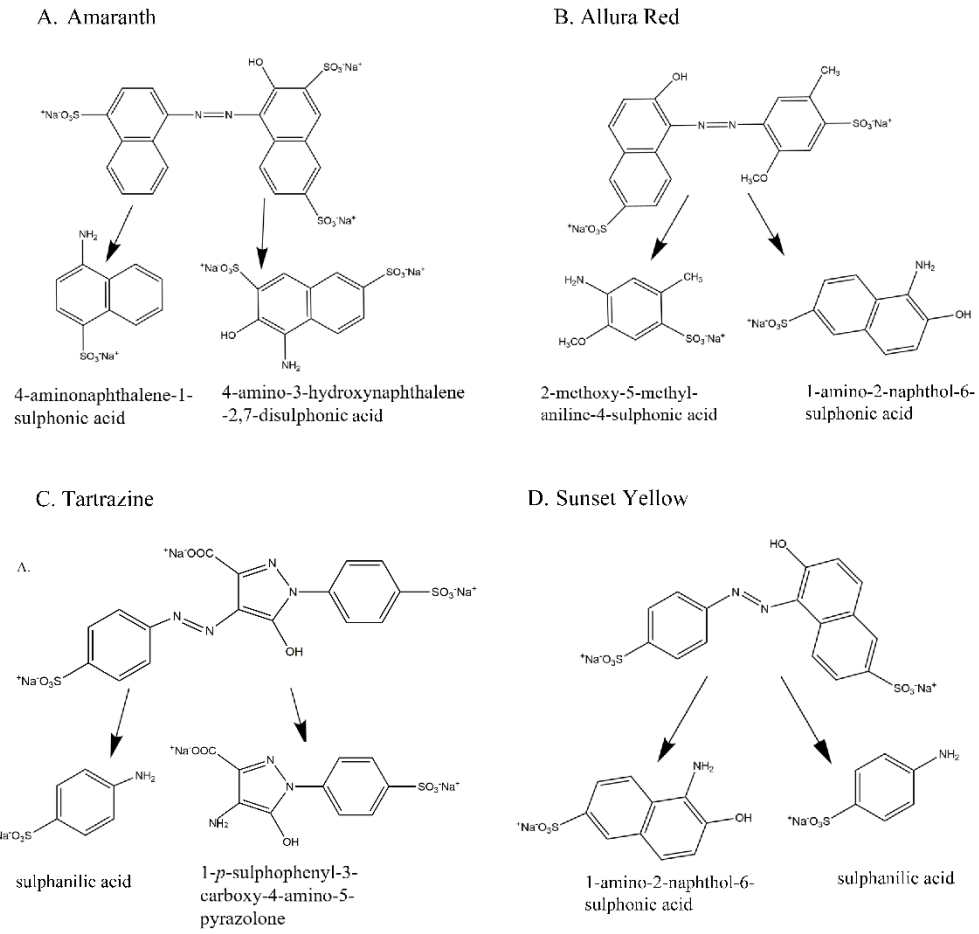

Figure 2.9: The metabolites produced from the azo reduction of the four food azo food dyes.

The data collected in the whole bacterial azo dye kinetics assays (Section 2.2.2) show that strains of the same species do not always reduce the same azo dyes. However, growth of a given strain has some impact on its ability to reduce different azo dyes. For example, the only *B. intestinihominis* strain to show any azo dye reduction, strain OB21 FMU 25, was also the only strain to show growth in the test medium. The strain *Odoribacter* sp. 21 D6 I showed growth, but not azo dye reduction, in BHI medium, which contrasted sharply with findings from the plate assay which demonstrated strong azo dye reduction by this strain on FAA medium. Thus, the

medium of growth could have caused the discrepancy in azo dye reduction seen between the plate assay and the whole cell kinetics, perhaps through the upregulation of azoreductase genes on one medium type but not the other.

Strains of the species *E. bolteae, C. symbiosum,* and *E. lavalensis* showed inhibited growth in the azo dye supplemented medium. This may have been a result of the reaction conditions in the polystyrene 96 well plate, or the azo dyes causing inhibition of growth. All of these species are from the *Eubacteriales* order which may explain the effects of the tested dyes on growth among these strains in the broth medium used (Figure 2.2). The *D. fastidiosa* strain 2 BHI does not show notable growth in BHI through the OD 600 nm readings, although its ability to reduce all four of the tested azo dyes is clear, Figure 2.8. However, the reduction of azo dyes by this strain follows a linear pattern rather than exponential, which may reflect the very minimal growth seen; use of a more optimal growth medium for this strain may have resulted in more rapid reduction of the azo dyes (Figure 2.7, Figure 2.8).

The growth of many bacterial species present in the human microbiome has been tested using the general method of measuring optical density of bacterial cells at 600 nm to determine the number of cells in a sample. Since optical density depends on the size of bacterial cells, and the range of bacterial cell sizes among the tested strains varies considerably, growth curve data can only be extrapolated reliably between the same species to determine changes in growth rather than enumerated total growth. The next step in determining whether species growth is affected by the azo dyes would be to standardize strain growth in BHI medium and test multiple biological replicates rather than technical replicates. If the azo dyes inhibit growth, then the mechanism of toxicity should be explored.

Azo dye toxicity towards bacterial cells could come from either the parent compound or the metabolites of dye reduction. Sunset Yellow and Tartrazine both produce sulphanilic acid as a reduction product (Figure 2.9). Sulphanilic acid does not readily degrade under anaerobic

conditions and may have detrimental effects on growth of bacteria[58,59]. Sulphanilic acid could be inhibiting growth of some species, such as *E. bolteae*, explaining the reduced reduction rate for Tartrazine and Sunset Yellow for most species. It would be interesting to see how the growth rate is affected by the metabolites. This could be explored by exposing bacterial species to various concentrations of e.g. sulphanilic acid and measuring the growth curves.

The two strains that showed increased growth in azo dye supplemented BHI medium when compared to the control were *C. innocuum* strain 5 FAA S (Appendix 2, Figure C) and *E. lenta* strain 25 D5 S (Figure 2.8). These two species reduced Sunset Yellow and Tartrazine fastest. Azo dyes or their metabolites may be a useful carbon source for these microbes; however, that was not tested in this work. *E. lenta* is well known for its ability to biotransform toxins, drugs and other xenobiotics. For example, it is able to modify digoxin to inactivate the compound[60]. *C. innocuum* is generally poorly studied, and although it is speculated to be an opportunistic pathogen, its biotransformative capabilities are unknown. Strains of the Lachnospiraceae species tested in this work, *C. symbiosum, E. bolteae H. effluvii*, *C. pacaense*, and *E. lavalensis,* similarly have never been tested for their biotransformative functions, although it has been suggested that some strains may perform bile acid transformations[61]. *Dielma fastidiosa* does not have any known reductase, oxidase, catalase, or biotransformation activity, so it is surprising that such strong azo dye reduction was seen with both *Dielma* strains tested[62].

A previous study, conducted in 2019, identified gut bacterial species with azoreductase capabilities, and, similar to the work presented here, showed strains of *O. splanchnicus* and *P. vulgatus* to reduce Allura Red and Sunset Yellow[54]. This previous research, however, showed different outcomes for tested strains of species including *Faecalicoccus* sp., *Dorea* sp., *Coprococcus comes*, *Eisenbergiella, Bacteroides uniformis, Collinsella aerofaciens, Bacteroides fragilis and ovatus, Clostridium hylemonae, Blautia* spp*. Ruminococcus faecis* and *Bifidobacterium* spp.[54], compared to strains tested in the work presented here. The differences

could be a result of the different media components used for strain growth, or the dye concentration; the assay carried out in this thesis deliberately used a higher concentration of azo dyes compared to the work of Zou *et al*.[54], in order to identify species that have relatively high azoreductase capabilities. Another explanation may be strain-to-strain variability.

2.5 Conclusion

The taxa exhibiting high azoreductase activity in this survey belonged to the genera *Clostridium, Hungatella, Enterocloster, Veillonella, Dielma, Eggerthella, Odoribacter*, and *Phocaeicola.* Overall, out of the four food azo dyes tested, Amaranth was reduced by the most bacterial species within the species isolated from the human gut microbiome, and Tartrazine by the fewest. Allura Red and Sunset Yellow have similar reduction rates; this seems to correlate to these dyes' structures. The growth of the bacterial strains that have azo dye reduction capabilities was affected by the presence of Sunset Yellow and Tartrazine in the BHI medium. The inhibited growth of these species could also explain why there was less reduction of these dyes under these circumstances. There could be multiple reasons for this inhibited growth, including insufficient nutrients in the BHI medium, and possible dye or metabolite toxicity. If azo dyes are consumed regularly by a host, they could affect the gut microbiome, and further work should focus on the response of gut microbial ecosystems to azo dyes and their reduction products.

3 Identification of Putative Azoreductase Enzymes

3.1 Introduction

Although azo dye reduction does occur within the human gut environment, the mechanisms remain unclear[1,3,63]. Azoreductase enzymes have been identified and structurally characterized in many aerobes and a few facultative anaerobes, but to date, none have been structurally characterized in commensal gut bacteria[1,11,43]. Azoreductase discovery in anaerobic

gut microbes could be limited by the unique conditions required for enzyme activity in an oxygen-free environment. As well, enzymes may be cryptic, with little identity to established bacterial azoreductases. Finally, the reduction of azo dyes in the gut environment may take place through a mechanism independent of azoreductases. Identifying enzymes that have the ability to reduce azo dyes, at the level demonstrated in whole bacterial cell kinetics, would support the concept that azo dye reduction in the gut microbiome is facilitated by azoreductase enzymes.

In chapter 2, it was shown that the *Veillonella* sp. strains 6_1_27 and 3_1_44 can reduce all four food azo dyes (Section 2.3), and these strains were thus selected to be screened for putative azoreductase enzymes. Candidate azoreductase enzymes present in the genomes of both strains were identified, expressed, and purified. Activity experiments were conducted to validate their capacity for reducing the four azo food dyes Amaranth, Allura Red, Sunset Yellow and Tartrazine under aerobic conditions.

3.2 Methods

3.2.1 Identifying Novel Azoreductase Enzymes; Construction of Expression Plasmids

The *Veillonella* sp. strains 6_1_27 and 3_1_44 have full genome sequence representation at a scaffold level assembly on NCBI. Database. These genomes were screened for azoreductase homologues by searching through predicted NAD(P)H-dependent oxidoreductase enzymes[64]. Known azoreductase genes, listed in Figure 3.1, were compared against the genome of strains 3_1 _44 and 6_1_27 using protein-protein BLAST (BLASTp)[64]. Genes encoding possible azoreductase enzymes were found. The genes were synthesized by Genscript and cloned into pET-28a+ plasmids using SacI/NdeI restraction sites. The genes were expressed via a pET-28a+ vector, including an N-terminal poly-histidine (His_6) tag. The structures and functions of the proteins (and structurally similar proteins) were predicted by the software I-TASSER[65 66]. Separately, the N-terminal his-tagged human NQO1 gene (hsNQO1) ORF was cloned into a pET-28b+ vector using NdeI restriction sites by our collaborators in the Ryan lab[67].

3.2.2 Protein Expression and Purification

Plasmids were transformed (heat-shock), into chemo-competent BL21 λDE3 *E. coli* cells. The cells were plated onto LB agar containing kanamycin (10 μg/ml) and incubated overnight at 37°C. A representative colony was inoculated into an aliquot (3 ml) of LB medium + kanamycin, 10 μg/ml, and incubated overnight at 37°C with shaking at 200 rpm. An aliquot (1 mL) of the overnight culture was inoculated into LB medium (100 mL, except 250 ml for vMdaB) containing kanamycin (10 μg/ml) and protein expression was induced at OD600 ~0.6 by the addition of IPTG (final concentration, 0.5 mM). After induction, cells were grown at 18°C, 200 rpm, for 16 h. Cells were harvested by centrifugation, 4,000 rpm, 15 min, at 4°C.

The cell pellet was resuspended in 10 mL of binding buffer containing 500 mM NaCl, 5 mM imidazole, and 25 mM Tris-HCl, pH 7.4 (Appendix 1). The resuspended cells were lysed by sonication (20 seconds on, 30 second off), for 10 cycles, on ice. The sonicated cells were centrifuged at 13,000 rpm for 30 min. Supernatants were pooled and incubated on ice for 10 min before protein purification. A chelating Fast Flow Sepharose column was charged with 50 mM nickel sulphate solution and then rinsed with binding buffer. The soluble fraction was added to the column, followed by 10 mL wash buffer (Appendix 1). Bound protein was eluted with elution buffer, 4 mL (Appendix 1). The eluate was collected in 0.5 ml fractions. Aliquots of the fractions were run on 10% acrylamide SDS-PAGE and the fractions containing the protein of interest were pooled.

3.2.3 Flavin Binding; Desalting

The protein of interest was incubated with 1 mM flavin (FAD or FMN) on ice, for at least 1 h. An Econo-Pac 10DG Desalting Columns gravity-flow desalting column (Bio-rad) was equilibrated with 25 mM Tris-HCl, pH 7.4. Protein was added to the column, followed by 5 mL of 25 mM Tris-HCl, pH 7.4. The eluted fractions were collected and analyzed on SDS-PAGE and fractions with abundant protein were pooled (Appendix 3). An absorbance spectrum was

recorded for analysis of final protein concentration. The flavin to protein absorbance percentage was calculated using $Absorbance\ \% = \frac{A450}{A280}(100)$. The extinction coefficients for the putative azoreductase apoenzymes were predicted using ExPASy[68] based on amino acid composition.

3.2.4 Enzyme Kinetics

All reagents were obtained from Sigma-Aldrich. The rates of substrate reduction were obtained by monitoring the decrease in absorbance at the absorbance peak for each azo dye (as stated in section 2.1.4, and at 600 nm for 2,6-dichlorophenolindophenol (DCPIP). Kinetic reactions were carried out in 1 ml reaction volume, using the Cary-UV 300 spectrophotometer and quartz cuvettes. The reactions were set up as follows: 100 mM NaCl, 300 mM NAD(P)H, 1-15 µg enzyme, in 25 mM Tris-HCl pH 7.4, 1 µM flavin (FAD or FMN), 40 µM dye substrate[40,67,69–72]. Initial rates of change were determined within 1 min. DCPIP extinction coefficient ε_{600} = 21 $mM^{-1}cm^{-1}$ [69,70,73]. The reaction was started by addition of enzyme. All dyes were prepared as 1 mM stocks in dH_2O. (Reactions with no enzyme, or no NADPH were used as controls).

3.3 Results

3.3.1 Identification of Putative Azoreductase Enzymes from *Veillonella* spp.

Two putative azoreductase genes were present in both the 3_1_44 and 6_1_27 genomes. These genes were annotated by NCBI Refseq. The gene vMdaB was predicted to have similar function to the MdaB (Modulator of Drug Activity B) gene and to be a putative NADPH-quinone reductase, and the second gene, vNfsB, was predicted to have a function similar to NfsB (Oxygen-insensitive Nitrofurazone/ Nitroreductase B) enzymes with an FMN binding region; Table 3.1[64]. Enzymes with known azoreductase and NQO reductase activity were used to identify similar genes/proteins in the *Veillonella* sp. genomes, and vMdaB was identified as a possible azoreductase analog, Table 3.1. vMdaB had amino acid sequence similarities of 31%

with efAzoR, 33% with ecAzoR, 31% with ecMdaB, 39% with paMdaB, 32% with paNQO1, and 32% with hsNQO1 (Figure 3.1). The vNfsB and the vMdaB sequences were aligned with known azoreductase and NQO enzymes and it was determined that vNfsB and vMdaB had sequences closer to azoreductase enzymes and NQO enzymes, respectively (Figure 3.1).

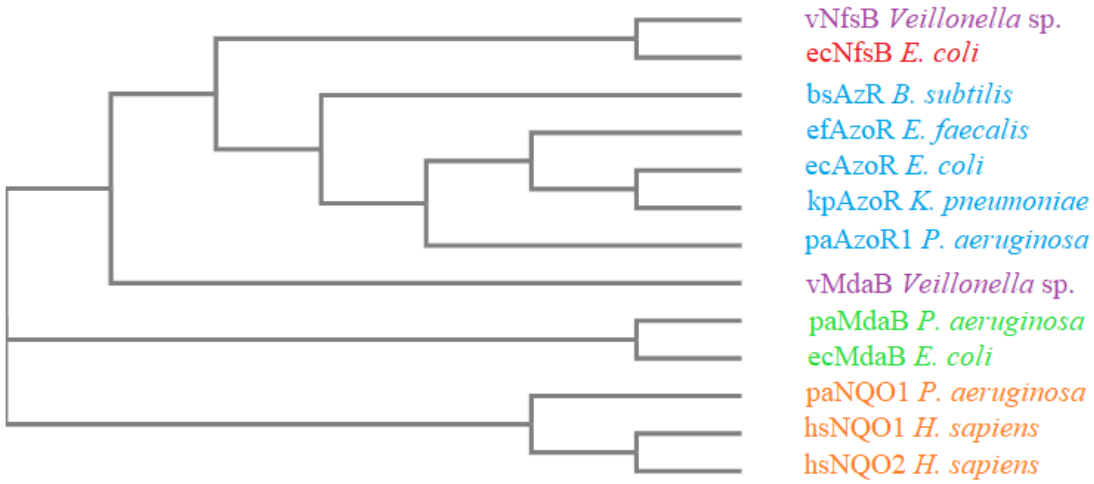

Figure 3.1: Phylogenetic tree illustrating relationships between known and putative azoreductase enzymes from *Veillonella* spp. An unrooted Phylip format neighbour-joining tree generated from the sequence alignment of 12 proteins by ClustalW. Proteins: blue, known bacterial azoreductase enzymes; green, known MdaB enzymes; orange, known NQO enzymes; red, *E. coli* NfsB; purple, putative *Veillonella* sp. azoreductase enzymes. efAzoR PBD: 2HPV, bsAzR PDB: 3W79, kpAzoR PDB: 6DXP, ecAzoR PDB: 2Z9D, paAzoR1 PDB: 2V9C, ecMdaB PDB: 2AMJ, paMdaB gene PA2580, paNQO1 gene PA1224, hsNQO2 PDB: 1SG0, and hsNQO1 PDB: 1D4A.

The structure of vMdaB was predicted to be similar to many azoreductase enzymes, including a putative oxidoreductase from *Streptococcus mutans*. PDB: 3LCM (RMSD = 0.53Å), hsNQO1 PDB: 1D4A (RMSD = 1.95Å), kpAzoR PDB: 6DXP (RMSD = 1.97Å), hsNQO2 PDB: 1SG0 (RMSD = 2.12Å), ecAzoR PDB 2Z9D (RMSD = 2.43Å), paAzoR1 PDB: 2V9C (RMSD = 2.51Å) and more, Figure 3.2. The structure of vNfsB was not predicted to be similar to

azoreductase enzymes; the top predicted analog was NAD(P)H-flavin oxidoreductase (NfoR) from *S. aureus* PDB: 7JH4 (RMSD = 0.92 Å), (Figure 3.2).

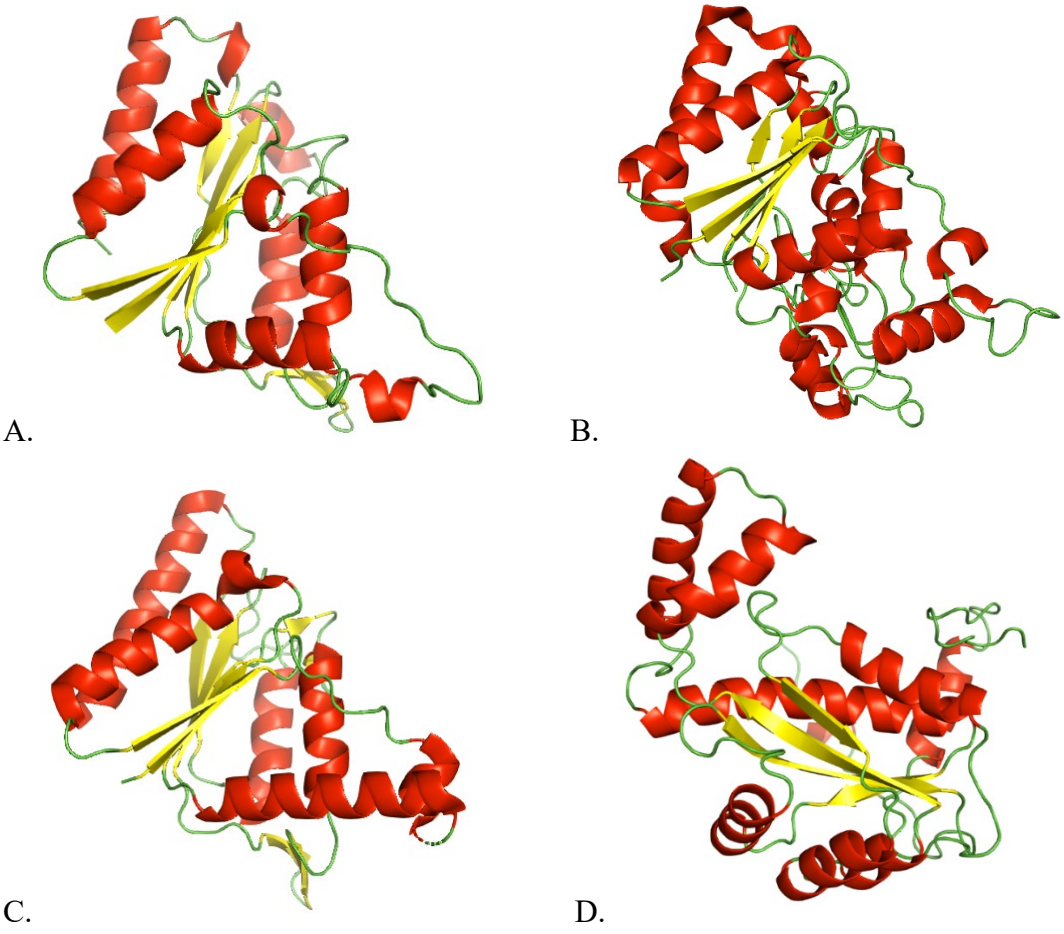

Figure 3.2: Monomers of characterized azoreductase enzymes A. ecAzoR (PDB: 2Z9D), B. hsNQO1 (PDB:1D4A), in relation to the I-TASSER predicted structure of putative *Veillonella* sp. azoreductase enzymes C. vMdaB, and D. vNfsB. (PyMOL)

3.3.2 Protein Isolation and Substrate Kinetics

The proteins used for kinetics assays are described in Table 3.1. After purification, the three enzymes were bound with either FAD or FMN and the percentage of flavin to protein

absorbance was calculated for each purification: $vMdaB_{FMN}$ = 56%, $vMdaB_{FAD}$ = 48%, $vNfsB_{FMN}$ = 41%, $vNfsB_{FAD}$ = 41%, and $hsNQO1_{FAD}$ = 50% (Figure 3.3).

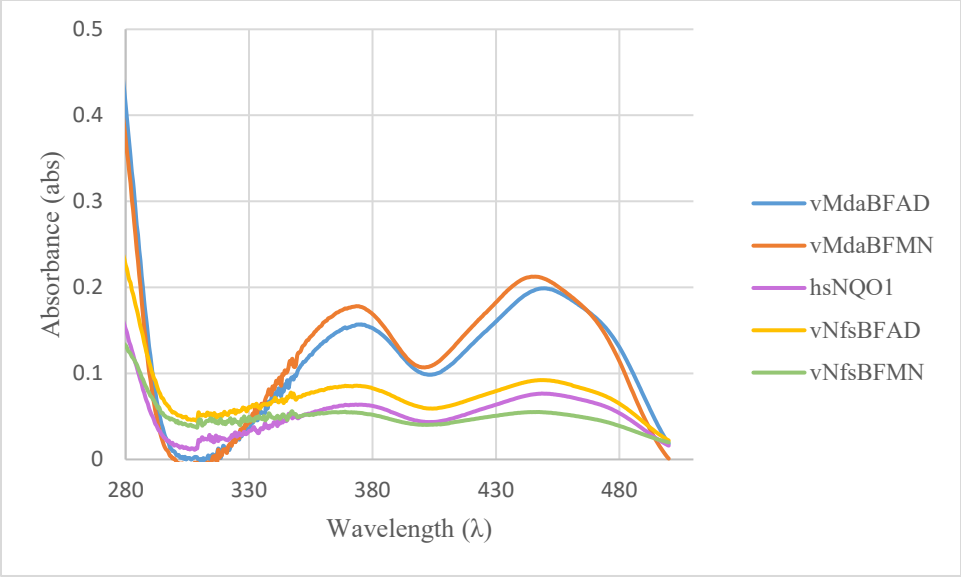

Figure 3.3: Absorbance spectra of proteins bound with flavin.

The substrate with highest specific activity for all enzymes listed in Table 3.1 was DCPIP. With the azo dye substrates, Amaranth, Allura Red, Sunset Yellow, and Tartrazine, reduction was detected but measured activity was not consistent under the conditions in section 3.1.4 were not obtained. The specific activity for $hsNQO1_{FAD}$ (774.4 nmol min^{-1} mg^{-1}) was ~4-fold lower than $vNfsB_{FAD}$ (3.28 µmol min^{-1} mg^{-1}) and ~13-fold lower than $vNfsB_{FMN}$ (10.0 µmol min^{-1} mg^{-1}). vNfsB with FMN had the most activity of all the flavin enzyme combinations and vNfsB had the second highest activity. The lowest enzyme activity with DCPIP was vMdaB. The vMdaB enzyme bound with FAD (138.3 nmol min^{-1} mg^{-1}) had ~1.4-fold higher activity than with FMN (99.0 nmol min^{-1} mg^{-1}).

Table 3.1: Amino acid sequences and predicted families of proteins used in enzyme activity assays.

Code	MW (kDa)	Species	Predicted Family	Amino acid sequence
hsNQO1	31	*Homo sapiens*	NAD(P)H dehydrogenase [quinone] 1 NAD(P)H: quinone oxidoreductase 1 (NQO1) Azoreductase	MVGRRALIVLAHSERTSFNYAMKEAAAA ALKKKGWEVVESDLYAMNFNPIISRKDIT GKLKDPANFQYPAESVLAYKEGHLSPDIV AEQKKLEAADLVIFQFPLQWFGVPAILKG WFERVFIGEFAYTYAAMYDKGPFRSKKA VLSITTGGSGSMYSLQGIHGDMNVILWPIQ SGILHFCGFQVLEPQLTYSIGHTPADARIQI LEGWKKRLENIWDETPLYFAPSSLFDLNF QAGFLMKKEVQDEEKNKKFGLSVGHHLG KSIPTDNQIKARK
vMdaB	22	*Veillonella* spp. (6_1_27 and 3_1_44)	Modulator of drug activity B (MdaB) NAD(P)H-dependent oxidoreductase	MNILIIYTYPNHQSFNDAILKVVQQNLSKD HNVNTLDLYEEQFDPIMRFDDTHKRRDLS TVPDMEKYRNLITWADQIIFIYPIWWSGM PAMLKGFIDRVFTAGFAYSYGKRGLIGHL QGKSAWIITTHNTPAFLTPFIQDYGKVLKN QVLKSCGIKPVTHTQLAGTENSSDEKRRR FLDKIANIAGSI
vNfsB	27	*Veillonella* spp. (6_1_27 and 3_1_44)	Nitroreductase (NfsB-like) NAD(P)H-dependent oxidoreductase	MSKYEIENVKLTAPKFDRKDLEYAMTYR YACKKFDSAKKISDDDWQGILTAARLSPT SLGFEAYQLLVIQNPEIREKMKAYGWGIQ AGLEASHFVVFLTRKKVDLEFDSPYVRYI QEEVKQLPAEVDAIYKEKYAQFTTEDYKT FESDRAAFDWSSKQAYIVMANMMTMAA YEGLDSCALEGFNQDKMTAFLGDELGLF DTKHFGIAVMAAFGYRDEEPHRNKTRRT MDEIVTVV

3.4 Discussion

The two putative *Veillonella* sp. azoreductase enzymes had activity with DCPIP, but no conclusive data was obtained for the four food azo dyes (section 3.1.4). The kinetics assays may not have been optimal for azo dye reduction; NAPDH was used as an electron donor and NADH has not been tested. Azoreductase enzymes have different hydride donor preferences, as described, for example, by Ryan *et al.*[40,67] . paAzoR1 showed preference for NADPH when reducing DCIP and methyl red; however, a homolog (paAzoR3) had a ~3-fold preference for

NADH[40]. Ryan *et al*. also found that substrate activity peaks at differing salt concentrations, ranging from 0.1-1M NaCl, which may need to be optimized for each enzyme[40]. The reaction conditions used here were chosen by combining protocols from published studies of ecAzoR, efAzoR, paAzoR1, and hsNQO1[40,67,69–72].

Based on the predicted structure, the enzyme vMdaB has a similar fold to many known azoreductases (Figure 3.2), and it was determined as most likely to be an azoreductase, among the annotated proteins encoded in the *Veillonella* sp. genome. The sequence similarity of vMdaB to other azoreductases is only about 30%. As with any enzyme protein, it is the tertiary structure - not just the amino acid sequence – that determines substrate binding[64].

The vNfsB enzyme had higher DCPIP reduction specific activity with either FMN or FAD than hsNQO1, for which DCIP is a known substrate. The enzyme ecNfsB also has DCPIP as a known substrate, so it was expected that the vNfsB would also be able to reduce the compound[74]. The vNfsB enzyme has ~ 3-fold higher activity for DCPIP with bound FMN vs. FAD.

The vMdaB enzyme has a very similar fold to hsNQO1 and, therefore, was a reasonable control to ensure that the purification and reaction conditions used allow for the reduction of DCPIP. Nevertheless, the low activity of vMdaB seen with DCPIP may mean that the purification conditions or reaction conditions were not optimal, and the enzyme may fold differently when expressed and purified under anaerobic conditions, i.e. closer to the native environment of the anaerobic bacterial source. There is a slight preference for activity with FAD vs FMN for vMdaB. Three-dimensional structures of vMdaB and vNfsB determined by X-ray crystallography would facilitate understanding of the binding sites and substrate specificities of the enzymes.

Most azoreductases that have been characterized and for which structures are available are from either aerobic or facultative anaerobes[1,11,40,47,69]. The putative NAD(P)H-dependent

oxidoreductase enzymes vNfsB and vMdaB derived from *Veillonella* spp., which are obligate anaerobic bacteria, have been confirmed to have oxidoreductase activity with both FMN and FAD as cofactors and NADPH as electron donor. Brown *et al*. demonstrated that a broth culture of *Veillonella parvula* can reduce Tartrazine and Sunset Yellow, but the enzyme responsible was not identified[51]. *Veillonella* spp. strains 3_1_44 and 6_1_27 have azo dye reduction properties when grown in the presence in azo dye media (section 2.2.2). It was hypothesized that vMdaB is the enzyme facilitating azo dye reduction of Amaranth, Allura Red, Sunset Yellow, and Tartrazine. NAD(P)H oxidoreductase enzymes from *Veillonella* sp. are functional under aerobic conditions, although their azoreductase activities remain to be characterized fully.

Our work was unable to show that this enzyme contributed to azo dye reduction under the tested conditions, and thus it remains unknown whether such reduction is caused by this or another, as yet determined enzyme, or another mechanism altogether. Another pathway for azo dye reduction is through hydrogen sulfide (H_2S) reduction of azo bonds[75]. This possibility was described in the work of Wolfson *et al.*, where H_2S generated from cysteine metabolism was shown to drive the reduction of Allura Red[75]. It was established (abiotically) that two molecules of H_2S transfer electrons to the azo-bond sequentially, resulting in bond cleavage[75]. *In vitro* experiments were conducted by growing *E. coli* in LB under anoxic conditions with no supplementation, or supplementation with serine or cysteine; the only condition that had complete azo dye reduction in < 10 hours was with cysteine supplementation; the conditions with only *E. coli* and LB showed no azo dye reduction[75]. The *in vivo* experiment involved mouse models given cysteine-rich diets dosed with Allura Red; when compared to the control, the mice fed Allura Red had decreased fecal sulfide levels[75]. This illustrates that, under the studied conditions, cysteine drives azo dye metabolism[75]. This paper has brought into question whether the major azo dye reduction pathway is azoreductase or H_2S facilitated[75].

3.5 Conclusion

Two putative azoreductase enzymes from the *Veillonella* sp. 3_1_44 and 6_1_27 can reduce DCPIP under aerobic conditions, but did not show clear evidence of reduction of Amaranth, Allura Red, Sunset Yellow, or Tartrazine. The enzyme vNfsB had high specific activity for DCPIP, with a flavin preference for FMN, and vMdaB had low specific activity with DCPIP and a slight flavin preference for FAD. The enzyme (or enzymes) that facilitates the azo dye reduction may be more cryptic that originally anticipated, or the reaction conditions may need to be modified in order for vMdaB or vNfsB to reduce azo dyes.

4 Future Directions and Conclusions

4.1 Azo Dye Metabolism in the Gut Microbiome

The results in this thesis demonstrate, through screening commensal human gut microbiome species, that Amaranth is the dye that is reduced most often, and Tartrazine is the dye that is reduced least often; out of the 133 isolates, 83 bacterial species tested for azo dye reduction 29 species were identified to have the ability to reduce Amaranth and only 15 were able to reduce Tartrazine. The species that demonstrated azo dye reduction belong to the multiple genera including *Clostridium, Hungatella, Enterocloster, Veillonella, Dielma, Eggerthella, Odoribacter*, and *Phocaeicola.* The growth of some bacterial strains was affected by the presence of Sunset Yellow and Tartrazine in BHI medium. Recently Wu *et al*. discovered that Tartrazine consumption under 10 mg/kg bw/day caused dysbiosis in the crucian carp gut microbiota[63]. After 2 months of treatment the crucian carp had increased oxidative stress and a change in histological structure of the intestine and liver[63]. The microbial communities changed significantly from the initial composition, when Tartrazine was consumed pathogenic microorganisms, such as *Bdellovibrio* and *Shewanella* were increased[63]. The next steps for investigating food azo dyes effects on microbial communities would be to simulate a human gut microbiome using a chemostat vessel and dose with Tartrazine to model the results of longer-

term consumption[57]. It is probable that azo dye consumption at the ADI may alter the abundance of certain species in a microbial community. This model could also be used to determine if ingesting multiple azo food dyes causes compounding effects, since ingesting several dyes and food additives would closer resemble typical human food consumption models.

Similarly, He *at al.* reported that the metabolites of Allura Red and Tartrazine induce colitis in mice over-expressing IL-23[20]. Previous clinical trials have shown ulcerative colitis, inflammatory bowel, and Crohn's disease can be effectively treated with IL-23 targeting therapies, although upregulation of IL-23 alone has not been shown to induce colitis in mice[20]. The metabolite that induced the relapse in colitis was 1-amino-2-naphthol-6-sulfonate sodium salt, which is a metabolite of Allura Red and Sunset Yellow[20]. The induction of colitis by Allura Red did not occur when the mice were given Allura Red prior to IL-23 over-expression, this may suggest an immunological tolerance to Allura Red is formed. An investigation into cytokine production from Allura Red and Tartrazine metabolites, including IL-23 provide a deeper insight into whether azo dyes, or their metabolites, play a role in stimulating inflammation. To study this in the context of human health, Caco-2 cells could be exposed to Allura Red, Tartrazine and their metabolites including Westöö's purple product, in order to test for cytokine production via an ELISA assay. If azo dyes are consumed regularly by a host, they could modify the gut microbiome, and further work should focus on the response of gut microbial ecosystems to azo dyes and their reduction products.

4.2 Identification of Putative Azoreductase Enzymes

Azoreductase enzymes have been identified in many aerobic and facultative anaerobic bacterial species. However, it is unlikely that these enzymes evolved to reduce azo bonds, since these bonds rarely occur in nature[40,67]. Azoreductase enzymes belong to a superfamily of oxidoreductases enzymes[40,67]. More research into the reduction of azo dyes by oxidoreductase enzymes could lead to identification of new azoreductase enzymes. Reduction by azoreductase

enzymes may not occur under aerobic conditions, which may require performing kinetics assays in anaerobic conditions, similar to reactions performed with *Clostridium perfringens*[43,44]. The putative *Veillonella* sp. azoreductase enzymes vNfsB and vMdaB could be investigated further with different reaction conditions and substrates to definitively confirm if these enzymes are able to reduce azo bonds. Even if either of these enzymes can reduce azo bonds, this enzyme may not catalyze the reduction of the four azo food dyes explored in this paper. Novel anaerobic bacterial species azoreductase enzymes could be cryptic and not like previously discovered enzymes, or the reaction may be facilitated by a compound like H_2S, as described by Wolfson *et al*.[75].

The mechanism of azo dye reduction by commensal gut microbiota species is still unknown. It is important to characterize the metabolites of food colourants, and to understand that the products created via biotransformation can have very different chemical and toxicological properties than the original structure. The four food azo dyes, Amaranth, Allura Red, Sunset Yellow, and Tartrazine, are consumed daily around the world; however, there is still controversy over the safety of these dyes. Gaining knowledge of the products of tartrazine metabolism and their toxicity is important for the health of humans and their microbiota.

References

1. Feng, J., Cerniglia, C. E. & Chen, H. Toxicological significance of azo dye metabolism by human intestinal microbiota. *Front Biosci (Elite Ed)* **4**, 568–568 (2012).

2. Amchova, P., Kotolova, H. & Ruda-Kucerova, J. Health safety issues of synthetic food colorants. *Regul Toxicol Pharmacol* **73**, 914–922 (2015).

3. Bafana, A., Devi, S. S. & Chakrabarti, T. Azo dyes: past, present and the future. *Environmental Reviews* **19**, 350–370 (2011).

4. Josephy, P. David & Mannervik, Bengt. *Molecular toxicology* **2** (Oxford University Press, 2006).

5. Ventura-Camargo, B. & Marin-Morales, M. Azo Dyes: characterization and toxicity- a review. *Textiles and Light Industrial Science and Technology* **2**, 85–103 (2013).

6. Kirk-Othmer Encyclopedia of Chemical Technology 4th **2** *Kirk-Othmer Encyclopedia of Chemical Technology* (2004).

7. Rafii, F., Hall, J. D. & Cerniglia, C. E. Mutagenicity of azo dyes used in foods, drugs and cosmetics before and after reduction by clostridium species from the human intestinal tract. *Food and Chemical Toxicology* **35**, 897–901 (1997).

8. Elbanna, K. *et al.* Microbiological, histological, and biochemical evidence for the adverse effects of food azo dyes on rats. *Journal of Food and Drug Analysis* **25**, 667–680 (2017).

9. Stolz, A. Basic and applied aspects in the microbial degradation of azo dyes. *Applied Microbiology and Biotechnology* **56**, 69–80 (2001).

10. Sharma, V., McKone, H. T. & Markow, P. G. A global perspective on the history, use, and identification of synthetic food dyes. *Journal of Chemical Education* **88**, 24–28 (2011).

11. Chung, K. T. Azo dyes and human health: a review. *Journal of Environmental Science and Health - Part C Environmental Carcinogenesis and Ecotoxicology Reviews* **34**, 233–261 (2016).

12. Miller, J. A. & Miller, E. C. The carcinogenicity of certain derivatives of p-dimethylaminozobenzene in the rat. *J Exp Med* **87**, 139–156 (1948).

13. Coultate, T. & Blackburn, R. S. Food colorants: their past, present and future. *Coloration Technology* **134**, 165–186 (2018).

14. Carliell, C. M., Barclay, S. J., Shaw, C., Wheatley, A. D. & Buckley, C. A. The effect of salts used in textile dyeing on microbial decolourisation of a reactive azo dye. *Environmental Technology (United Kingdom)* **19**, 1133–1137 (1998).

15. Khayyat, L., Essawy, A., Sorour, J. & Soffar, A. Tartrazine induces structural and functional aberrations and genotoxic effects in vivo. *PeerJ* **5**, e3041 (2017).

16. Sweeney, E. A., Chipman, J. K. & Forsythe, S. J. Evidence for direct-acting oxidative genotoxicity by reduction products of azo dyes. *Environmental Health Perspectives* **102**, 119–122 (1994).

17. Shimada, C., Kano, K., Sasaki, Y. F., Sato, I. & Tsudua, S. Differential colon DNA damage induced by azo food additives between rats and mice. *Journal of Toxicological Sciences* **35**, 547–554 (2010).

18. Tsuda, S. *et al.* DNA damage induced by red food dyes orally administered to pregnant and male mice. *Toxicological Sciences* **61**, 92–99 (2001).

19. Vorhees, C. v., Butcher, R. E., Brunner, R. L., Wootten, V. & Sobotka, T. J. Developmental toxicity and psychotoxicity of FD and C red dye no. 40 (Allura red AC) in rats. *Toxicology* **28**, 207–217 (1983).

20. He, Z. *et al.* Food colorants metabolized by commensal bacteria promote colitis in mice with dysregulated expression of interleukin-23. *Cell Metabolism* **33**, 1358–1357 (2021).

21. Feingold, B. F. Hyperkinesis and learning disabilities linked to artificial food flavors and colors. *American Journal of Nursing* **75**, 797–803 (1975).

22. McCann, D. *et al.* Food additives and hyperactive behaviour in 3-year-old and 8/9-year-old children in the community: a randomised, double-blinded, placebo-controlled trial. *Lancet* **370**, 1560–1567 (2007).

23. El-Borm, H., Badawy, G., Hassab El-Nabi, S., El-Sherif, W. & Atallah, M. Toxicity of Sunset Yellow FCF and Tartrazine dyes on DNA and cell cycle of liver and kidneys of the chick embryo: the alleviative effects of curcumin. *Egyptian Journal of Zoology* **74**, 43–55 (2020).

24. Scientific opinion on the re-evaluation of Sunset Yellow FCF (E 110) as a food additive. *EFSA Journal* **7**, 1330 (2009).

25. Boussada, M. *et al.* Assessment of a sub-chronic consumption of tartrazine (E102) on sperm and oxidative stress features in Wistar rat. *International Food Research Journal* **24**, 1473–1481 (2017).

26. Elhkim, M. O. *et al.* New considerations regarding the risk assessment on Tartrazine. An update toxicological assessment, intolerance reactions and maximum theoretical daily intake in France. *Regulatory Toxicology and Pharmacology* **47**, 308–316 (2007).

27. Juhlin, L., Michaëlsson, G. & Zetterström, O. Urticaria and asthma induced by food-and-drug additives in patients with aspirin hypersensitivity. *The Journal of Allergy and Clinical Immunology* **50**, 92–98 (1972).

28. Giri, A. K., Das, S. K., Talukder, G. & Sharma, A. Sister chromatid exchange and chromosome aberrations induced by curcumin and tartrazine on mammalian cells in vivo. *Cytobios* **62**, 111–117 (1990).

29. Durnev, A. D., Oreshchenko, A. v., Kulakova, A. v. & Beresten', N. F. Analysis of cytogenetic activity of food dyes. *Voprosy meditsinskoi khimii* **41**, 50–53 (1995).

30. Westöö, G. On the metabolism of tartrazine in the rat. *Acta Chem Scand* **19**, 1309–1316 (1965).

31. Pérez-Díaz, I. M. & McFeeters, R. F. Modification of azo dyes by lactic acid bacteria. *Journal of Applied Microbiology* **107**, 584–589 (2009).

32. Chung, K. T., Fulk, G. E. & Egan, M. Reduction of azo dyes by intestinal anaerobes. *Appl Environ Microbiol* **35**, 558–562 (1978).

33. Robinson, T., McMullan, G., Marchant, R. & Nigam, P. Remediation of dyes in textile effluent: A critical review on current treatment technologies with a proposed alternative. *Bioresource Technology* **77**, 247–255 (2001).

34. Crescente, V. *et al.* Identification of novel members of the bacterial azoreductase family required for infection of mammals by *Pseudomonas aeruginosa*. *Biochemical Journal* **473**, 549–558 (2016).

35. Chen, H. Recent advances in azo dye degrading enzyme research. *Current Protein & Peptide Science* **7**, 101–111 (2006).

36. Chen, H., Feng, J., Kweon, O., Xu, H. & Cerniglia, C. E. Identification and molecular characterization of a novel flavin-free NADPH preferred azoreductase encoded by azoB in *Pigmentiphaga kullae* K24. *BMC Biochemistry* **11**, 13 (2010).

37. Chen, H., Hopper, S. L. & Cerniglia, C. E. Biochemical and molecular characterization of an azoreductase from *Staphylococcus aureus*, a tetrameric NADPH-dependent flavoprotein. *Microbiology (N Y)* **151**, 1433–1441 (2005).

38. Misal, S. A. & Gawai, K. R. Azoreductase: a key player of xenobiotic metabolism. *Bioresources and Bioprocessing* **5**, 1–9 (2018).

39. Chen, H., Xu, H., Kweon, O., Chen, S. & Cerniglia, C. E. Functional role of Trp-105 of *Enterococcus faecalis* azoreductase (AzoA) as resolved by structural and mutational analysis. *Microbiology (N Y)* **154**, 2659–2667 (2008).

40. Ryan, A., Wang, C., Laurieri, N., Westwood, I. & Sim, E. Reaction mechanism of azoreductases suggests convergent evolution with quinone oxidoreductases. *Protein and Cell* **1**, 780–790 (2010).

41. Blümel, S., Knackmuss, H. J. & Stolz, A. Molecular cloning and characterization of the gene coding for the aerobic azoreductase from *Xenophilus azovorans* KF46F. *Applied and Environmental Microbiology* **68**, 3948–3955 (2002).

42. Rafii, F., Franklin, W. & Cerniglia, C. E. Azoreductase activity of anaerobic bacteria isolated from human intestinal microflora. *Applied and Environmental Microbiology* **56**, (1990).

43. Morrison, J. *et al.* Structure and stability of an azoreductase with an FAD cofactor from the strict anaerobe *Clostridium perfringens*. *Protein & Peptide Letters* **21**, 523–534 (2014).

44. Morrison, J. M. & John, G. H. Non-classical azoreductase secretion in *Clostridium perfringens* in response to sulfonated azo dye exposure. *Anaerobe* **34**, 34–43 (2015).

45. Rafii, F. & Cerniglia, C. E. Localization of the azoreductase of *Clostridium perfringens* by immuno-electron microscopy. *Current Microbiology* **27**, 143–145 (1993).

46. Dethlefsen, L., McFall-Ngai, M. & Relman, D. A. An ecological and evolutionary perspective on human-microbe mutualism and disease. *Nature* **449**, 811–818 (2007).

47. Bafana, A. & Chakrabarti, T. Lateral gene transfer in phylogeny of azoreductase enzyme. *Computational Biology and Chemistry* **32**, 191–197 (2008).

48. Collier, S. W., Storm, J. E. & Bronaugh, R. L. Reduction of azo dyes during in vitro percutaneous absorption. *Toxicology and Applied Pharmacology* **118**, 73–79 (1993).

49. Koppel, N., Rekdal, V. M. & Balskus, E. P. Chemical transformation of xenobiotics by the human gut microbiota. *Science* **356**, e2770 (2017).

50. Russ, R., Rau, J. & Stolz, A. The function of cytoplasmic flavin reductases in the reduction of azo dyes by bacteria. *Applied and Environmental Microbiology* **66**, 1429–1434 (2000).

51. Brown, J. P. Reduction of polymeric azo and nitro dyes by intestinal bacteria. *Applied and Environmental Microbiology* **41**, 1283–1286 (1981).

52. Eckburg, P. B. *et al.* Diversity of the human intestinal microbial flora. *Science (1979)* **308**, 1635–1638 (2005).

53. Kumaran, S., Ngo, A. C. R., Schultes, F. P. J., Saravanan, V. S. & Tischler, D. In vitro and in silico analysis of Brilliant Black degradation by *Actinobacteria* and a *Paraburkholderia* sp. *Genomics* **114**, e110266 (2022).

54. Zou, L. *et al.* Bacterial metabolism rescues the inhibition of intestinal drug absorption by food and drug additives. *Proc Natl Acad Sci U S A* **117**, 16009–16018 (2020).

55. Vacca, M. *et al.* The controversial role of human gut lachnospiraceae. *Microorganisms* **8**, 573 (2020).

56. Schoch, C. L. *et al.* NCBI Taxonomy: A comprehensive update on curation, resources and tools. *Database* **2020**, (2020).

57. McDonald, J. A. K. *et al.* Evaluation of microbial community reproducibility, stability and composition in a human distal gut chemostat model. *Journal of Microbiological Methods* **95**, 167–174 (2013).

58. Mezohegyi, G. *et al.* Effective anaerobic decolorization of azo dye acid orange 7 in continuous upflow packed-bed reactor using biological activated carbon system. in *Industrial and Engineering Chemistry Research* **46,** 6788–6792 (2007).

59. Topaç, F. O., Dindar, E., Uçaroğlu, S. & Başkaya, H. S. Effect of a sulfonated azo dye and sulfanilic acid on nitrogen transformation processes in soil. *Journal of Hazardous Materials* **170**, 1006–1013 (2009).

60. Koppel, N., Bisanz, J. E., Pandelia, M. E., Turnbaugh, P. J. & Balskus, E. P. Discovery and characterization of a prevalent human gut bacterial enzyme sufficient for the inactivation of a family of plant toxins. *Elife* **7**, (2018).

61. Lucas, L. N. *et al.* Dominant bacterial phyla from the human gut show widespread ability to transform and conjugate bile acids. *mSystems* **6**, (2021).

62. Ramasamy, D., Lagier, J. C., Nguyen, T. T., Raoult, D. & Fournier, P. E. Non contiguous-finished genome sequence and description of *Dielma fastidiosa* gen. nov., sp. nov., a new member of the Family Erysipelotrichaceae. *Standards in Genomic Sciences* **8**, 336–351 (2013).

63. Wu, L. *et al.* Impacts of an azo food dye tartrazine uptake on intestinal barrier, oxidative stress, inflammatory response and intestinal microbiome in crucian carp (*Carassius auratus*). *Ecotoxicology and Environmental Safety* **223**, e112551 (2021).

64. Altschul, S. F. *et al.* Gapped BLAST and PSI-BLAST: a new generation of protein database search programs. *Nucleic Acids Research* **25**, 3389–3402 (1997).

65. Yang, J. & Zhang, Y. I-TASSER server: New development for protein structure and function predictions. *Nucleic Acids Research* **43**, 174–181 (2015).

66. Zhang, C., Freddolino, P. L. & Zhang, Y. COFACTOR: Improved protein function prediction by combining structure, sequence and protein-protein interaction information. *Nucleic Acids Research* **45**, 291–299 (2017).

67. Ryan, A. *et al.* Identification of NAD(P)H quinone oxidoreductase activity in azoreductases from *P. aeruginosa*: Azoreductases and NAD(P)H quinone oxidoreductases belong to the same FMN-dependent superfamily of enzymes. *PLoS ONE* **9**, (2014).

68. Gasteiger, E. *et al.* ExPASy: the proteomics server for in-depth protein knowledge and analysis. *Nucleic Acids Research* **31**, 3784–3788 (2003).

69. Hollander, P. M. & Ernster, L. Studies on the reaction mechanism of DT diaphorase. Action of dead-end inhibitors and effects of phospholipids. *Archives of Biochemistry and Biophysics* **169**, 560–567 (1975).

70. Bongard, R. D. *et al.* Characterization of the threshold for NAD(P)H:quinine oxidoreductase (NQO1) activity in intact sulforaphane treated pulmonary arterial endothelial cells. *Free Radic Biol Med* **50**, 953–962 (2011).

71. Chalansonnet, V., Mercier, C., Orenga, S. & Gilbert, C. Identification of *Enterococcus faecalis* enzymes with azoreductases and/or nitroreductase activity. *BMC Microbiology* **17**, 126 (2017).

72. Liu, G., Zhou, J., Fu, Q. S. & Wang, J. The *Escherichia coli* azoreductase AzoR is involved in resistance to thiol-specific stress caused by electrophilic quinones. *Journal of Bacteriology* **191**, 6394–6400 (2009).

73. Hall, B. S., Meredith, E. L. & Wilkinson, S. R. Targeting the substrate preference of a type I nitroreductase to develop antitrypanosomal quinone-based prodrugs. *Antimicrob Agents Chemother* **56**, 5821–5830 (2012).

74. Zenno, S., Koike, H., Tanokura, M. & Saigo, K. Gene cloning, purification, and characterization of NfsB, a minor oxygen-insensitive nitroreductase from *Escherichia coli*, similar in biochemical properties to FRase I, the major flavin reductase in *Vibrio fischeri*. *Journal of Biochemistry* **120**, 736–744 (1996).

75. Wolfson, S. *et al.* Microbial cysteine degradation drives cryptic sulfide redox chemistry in the gut. *In Press* 1–21 (2021) doi:10.21203/rs.3.rs-909548/v1.

Appendix 1 - Buffers and Media

Freezing medium

60.0g skim milk powder

5 ml DMSO

5 ml Glycerol

490 ml ddH_2O

Binding Buffer (pH 7.4)

500 mM NaCl

5 mM imidazole

25 mM Tris-HCl

Wash Buffer (pH 7.4)

500 mM NaCl

60 mM imidazole

25 mM Tris-HCl

Elution Buffer (pH 7.4)

500 mM NaCl

500 mM imidazole

25 mM Tris-HCl

Appendix 2 – Growth curves

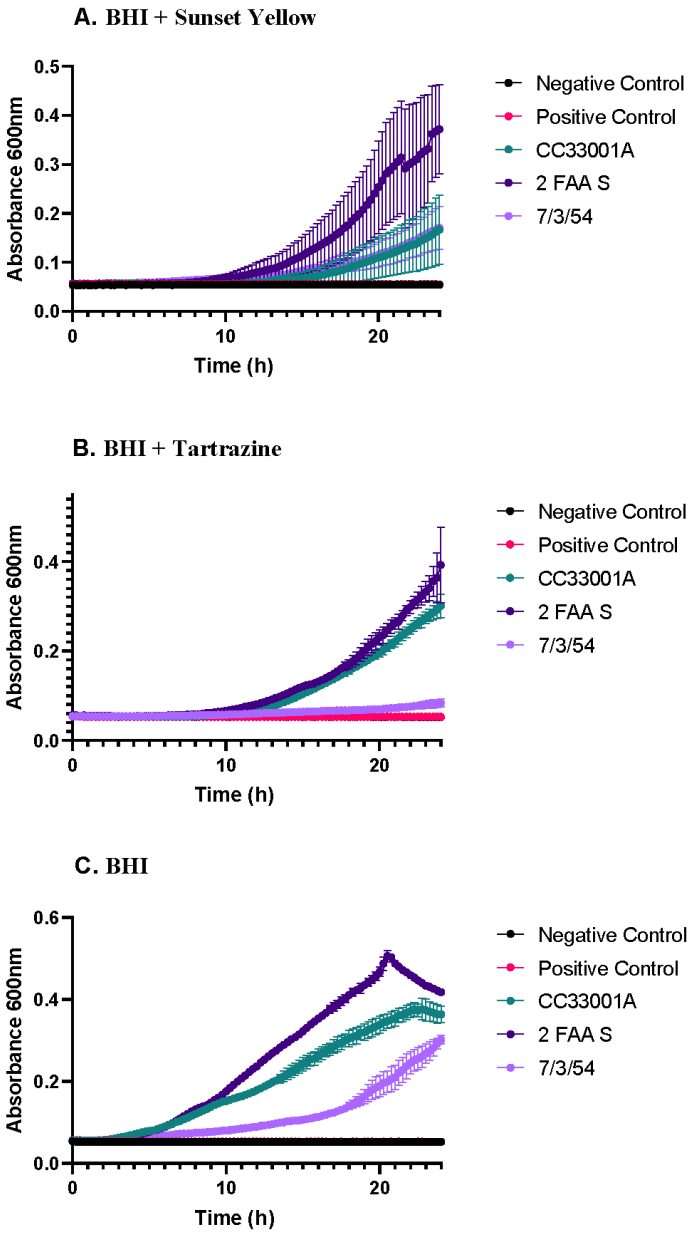

Figure A: 24 h incubation of *C. symbiosum* strains CC33001A, 2 FAA S, and 7/3/54, at 37°C under anaerobic conditions. The growth of these strains was measured in BHI or BHI media supplemented with 250 µM azo dye.

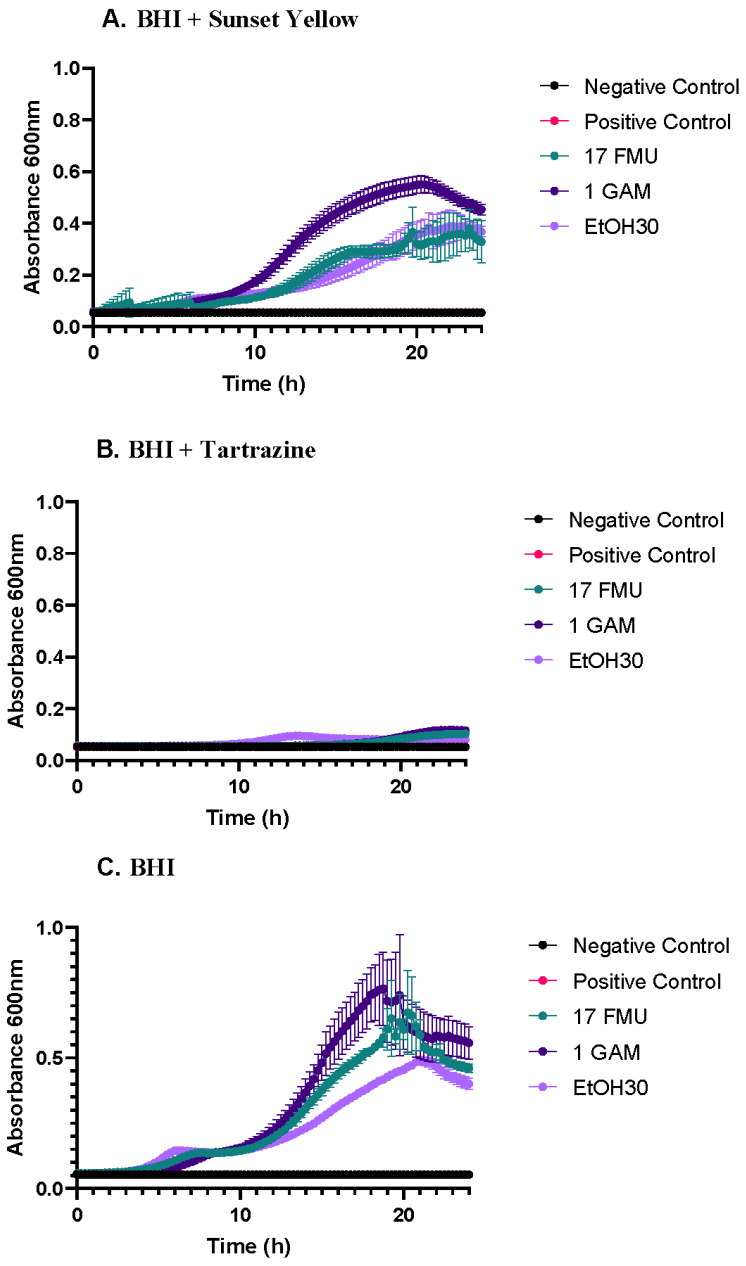

Figure B: The 24 h incubation of *E. bolteae* strains17 FMU, 1 GAM, and EtOH30, at 37°C under anaerobic conditions. The growth of these strains was measured in BHI or BHI media supplemented with 250 µM azo dye.

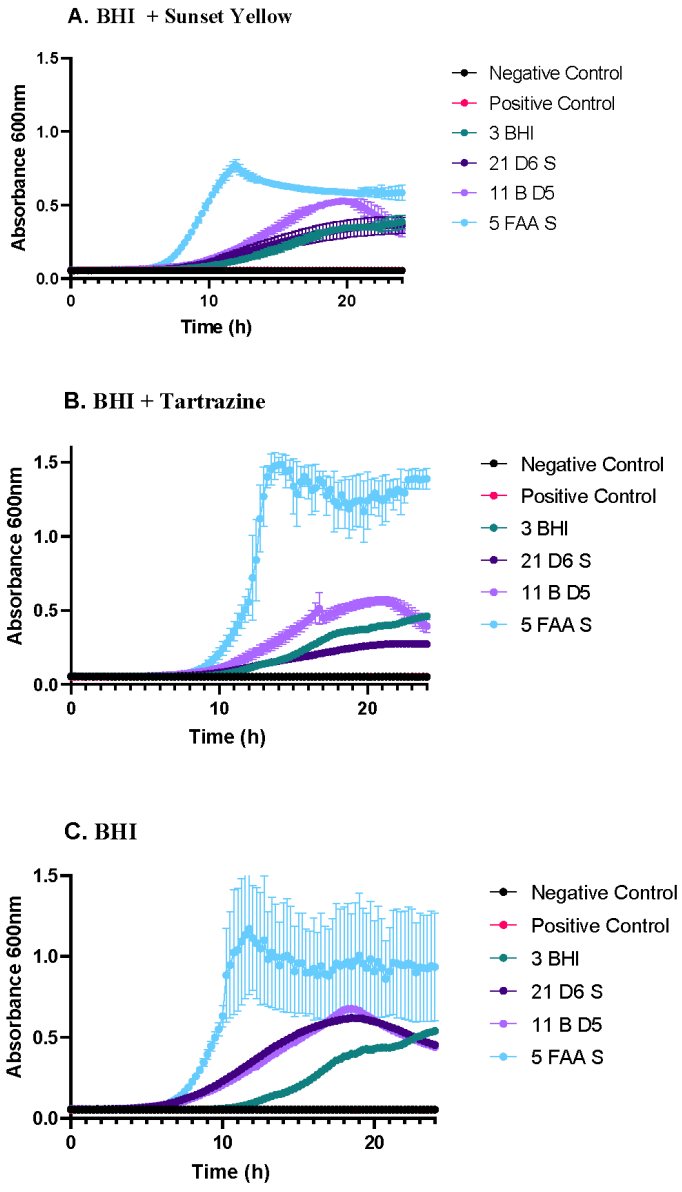

Figure C: The 24 h incubation of *H. effluvii* strain 3 BHI, *C. pacaense* strain 21 D6 S, *E. lavalensis* strain 11 B D5, *C. innocuum* strain 5 FAA S, *D. fastidiosa* strain 2 BHI, and *E. lenta*

strain 25 D5 S, at 37°C under anaerobic conditions. The growth of these strains was measured in BHI or BHI media supplemented with 250 µM azo dye.

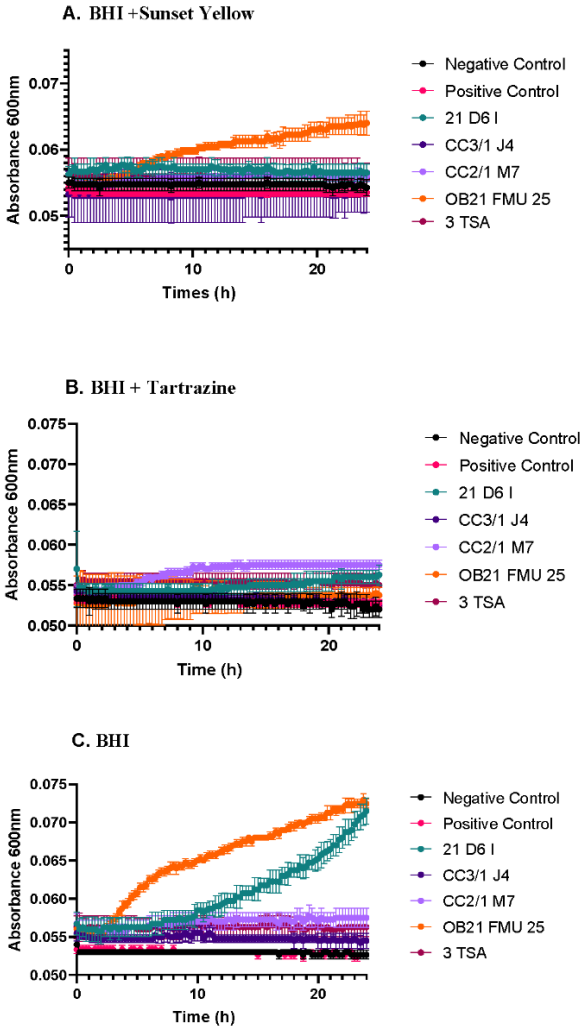

Figure D: Growth during 24 h incubation period for *Odoribacter* sp. strain 21 D6 I, *Barnesiella* spp. strains CC3/1 J4, CC2/1 M7 and OB21 FMU 25, and *Phocaeicola* sp. strain 3 TSA, at 37°C under anaerobic conditions. The growth of these strains was measured in BHI or BHI media supplemented with 250 µM azo dye.

Appendix 3 – vNfsB, vMDaB and hsNQO1 proteins

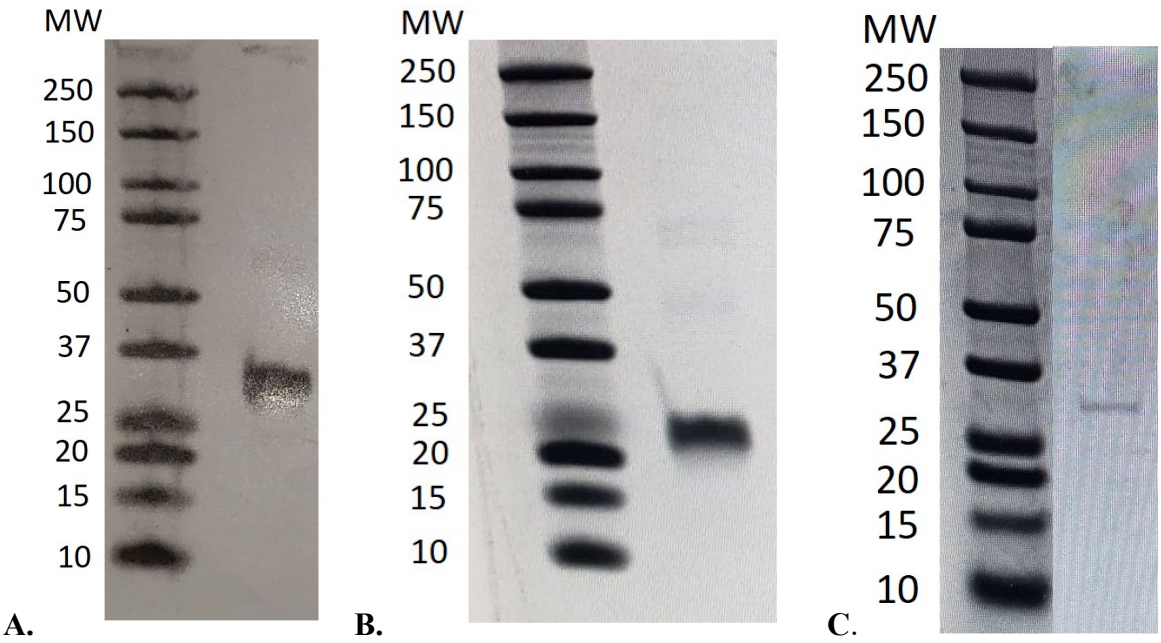

Figure E: SDS-PAGE image of fractions collected after flavin-bound protein was added to a gravity flow desalting column (Bio-rad). The column was equilibrated with 25 mM Tris-HCl, pH 7.4, then protein was added to the column, followed by 5 mL of 25 mM Tris-HCl, pH 7.4. The eluted fractions were collected and analyzed on SDS-PAGE. The proteins were compared against Bio-rad Precision Plus protein standard. (A) vNfsB protein bound with FMN, (B) vMdaB protein bound with FAD, and (C) hsNQO1 protein bound with FAD.